Boston University Theses & Dissertations

2014

Preliminary investigation of acute recovery and the influence of anesthetics following blast induced traumatic brain injury in C57BL/6 mice

BOSTON UNIVERSITY

GRADUATE SCHOOL OF ARTS AND SCIENCES

Thesis

PRELIMINARY INVESTIGATION OF ACUTE RECOVERY AND THE INFLUENCE OF ANESTHETICS FOLLOWING BLAST INDUCED TRAUMATIC BRAIN INJURY IN C57BL/6 MICE

by

GLORIA JESSICA DeWALT

B.S., Dickinson College, 2007

Submitted in partial fulfillment of the

requirements for the degree of

Master of Arts

2014

Approved by

First Reader
William D. Eldred, PhD
Professor of Biology

Second Reader
Jen-Wei Lin, PhD
Associate Professor of Biology

Third Reader
Vincent E. Dionne, PhD
Professor of Biology

Acknowledgements

I cannot think of a more appropriate story to describe my graduate experience:

One night I dreamed a dream. I was walking along the beach with my Lord. Across the dark sky flashed scenes from my life. For each scene, I noticed two sets of footprints in the sand, one belonging to me and one to my Lord. When the last scene of my life shot before me I looked back at the footprints in the sand and to my surprise, I noticed that many times along the path of my life there was only one set of footprints. I realized that this was at the lowest and saddest times of my life. This always bothered and I questioned the Lord about my dilemma.

"Lord, you told me when I decided to follow You, You would walk and talk with me all the way. But I'm aware that during the most troublesome times of my life there is only one set of footprints. I just don't understand why, when I needed You most, You leave me."

He whispered, "My precious child, I love you and will never leave you never, ever during your trials and testings. When you saw only one set of footprints it was then that I carried you."

-Margaret Fishback Powers, Footprints 1964

I would like to thank my mother, Veronica Small, and my sister, Monica DeWalt for always reminding me about the bright side of life as well as my best friend, Andreas Eleftheriou, DVM who routinely reminded me that I am loved.

Many thanks to my advisor, Bill Eldred, a very caring mentor. Your patience, confidence, sense of humor, and availability whenever I needed help made working in your lab a great experience. I will always be grateful to Todd Blute, a great mentor and brilliant scientist, who helped me recognize the importance of good science, attention to details and always provided sound advice.

Without the help of my committee this thesis would not have been completed. Thank you, Dr. Dionne for taking the time to help and advise me objectively. Thank you, Dr. Lin for always helping me, patiently listening to my antics and being a great mentor.

I would not have transitioned into leading the lab without the kind mentorship of Jan Blom and friendship from Shirley Sanchez. To my former labmates: Vanessa Hill, Fatema-Zahra El Rhermoul, Jason Thai, Ploy Ploysangam, Lauren Thompson and Andrew Marttini, I have such wonderful memories with each of you that I will cherish. To my current labmates: Andrea Foster, Dwayne D'Souza, Xiao Gao, Micaela Gobielle, Shama Patel, Amber Thiel and Chris Brooks thanks for making lab so enjoyable. In particular thank you, Andrea, for your work in calibrating data used in my thesis. Dwayne and Xiao thank you for your help whenever I needed it and for always checking in with me and being good company, I really appreciate it. Ellen Witkowski, thank you for being a great friend and collaborator. I would also like to thank all other members of the Davison lab (Yuan, Linnea and Ian) for their insight and many of the animals used in this thesis.

Many of the positive experiences I have had at BU center around the opportunity to teach. This would not have been possible without Meredith Canode. Thank you, Meredith, for your help, saavy, and fun stories. Special thanks to Dr. Kathyrn Spilios for showing me how wonderful and fulfilling teaching can be as well as all of my former students.

The support and motivation from friends at BU, particularly Shannon Kordus, Kristina Cohen, Lauren Tereshko, Liz McCarthy, Julia Kerner, and Jeff Markowitz, among many others, has helped me so much during my masters. I look forward to keeping in touch.

And lastly, a special thanks to two of the greatest Shih Tzus I have had the pleasure of knowing, Maggie and Ella-Lena, who stayed up with me during many late nights of studying and thesis writing always motivating me to keep going and reminding me to take a break for important things like tummy rubs, hugs and hilarious games of fetch!

PRELIMINARY INVESTIGATION OF ACUTE RECOVERY AND THE INFLUENCE OF ANESTHETICS FOLLOWING BLAST INDUCED TRAUMATIC BRAIN INJURY IN C57BL/6 MICE

GLORIA JESSICA DEWALT

ABSTRACT

Recognition of traumatic brain injury (TBI) has increased due to higher rates of injuries reported in sports and veterans. Several animal models exist to study TBI, but one that is particularly relevant in recapitulating combat trauma is blast-induced TBI (bTBI). Ethical considerations have resulted in the use of anesthetics and analgesics in virtually all animal models of TBI. However, emerging evidence indicates that anesthetics may provide neuroprotection that could confound results. Therefore, I am determining the level of anesthetic induced neuroprotection in acute recovery (48 Hours) following bTBI by assessing damage sustained to the dentate gyrus, retrosplenial and visual cortices. Using a Cranium Only Blast Injury Apparatus, I delivered non-lethal blast overpressures averaging 534 kiloPascals (kPa) to five groups of adult C57BL/6 mice (control, no anesthetic, xylazine only (13 mg/kg, IP), xylazine/buprenorphine (13 mg/kg, IP and 0.1 mg/kg, SC), and ketamine, xylazine, buprenorphine (75 mg/kg, IP, 13 mg/kg, IP 0.1 mg/kg, SC). Following recovery, immunocytochemistry was used to visualize changes in: doublecortin (a marker for neurogenesis), parvalbumin and calretinin (two calcium-binding proteins), and the astrocytic marker glial fibrillary acidic protein. My preliminary results show increases in neurogenesis and differential effects of calretinin and parvalbumin in all brain regions following blast injury in the absence of anesthetic and that the use of anesthetics alters these results. Because injuries sustained in combat

may not receive medical attention until 48 hours after trauma, this time point can offer valuable information regarding the specific pathways affected and the therapeutic window required for pharmacological intervention.

TABLE OF CONTENTS

List of Tables

List of Figures

List of Abbreviations

bTBI	blast-induced Traumatic Brain Injury
CCI	Control Cortical Impact
CR	Calretinin
CT	Computed tomography
DAI	Diffuse Axonal Injury
DG	Dentate gyrus
FPI	Fluid Percussion Injury
GCS	Glasgow coma scale
GFAP	Glial fibrillary acidic protein
NMDA	N-methyl-D-aspartate
PTSD	Post Traumatic Stress Disorder
PV	Parvalbumin
RSC	Retrosplenial cortex
TAI	Traumatic axonal injury
TBI	Traumatic Brain Injury

Chapter 1

INTRODUCTION

What is traumatic brain injury?

Traumatic brain injury (TBI) is used to define a complex series of events leading to brain damage (Morales *et al.*, 2005, Xiong *et al.*, 2013, Kan *et al.*, 2012). Cited as a silent epidemic that causes non-lethal yet significant disabilities worldwide, it has been reported that every 23 seconds in the US a person suffers from TBI resulting in significant cognitive defects (Bonislawski *et al.*, 2007, Morales et al., 2005). Symptoms of TBI result primarily from damage due to external mechanical force. Examples of such force include: blast waves, projectile impact and rapid acceleration/deceleration (Cernak *et al.*, 1999). The primary damage sustained during TBI progresses into secondary injury that culminates in irreversible cognitive and physical impairments (Blennow *et al.*, 2012). Key facets of secondary injury have included: excitotoxicity due to excessive release of excitatory transmitters, calcium influxes, increased production of free radicals and cytokines, mitochondrial damage, and changes in expression of transcription factors, inflammatory mediators and neuroprotective genes (Xiong et al., 2013). The overall goal in TBI research is to understand its underlying pathology in order to fully identify secondary events responsible for the associated cognitive and physical deficits.

Brief historical review of TBI

Although much of the recent emphasis regarding TBI is focused on combat and sports, the earliest account of blast injury dates back to 1768 when mining accidents in Northern England were prevalent (Jars, 1768). Work published by M Jars detailed the ability to survive “bad air” following explosions in mines by orientating oneself in a supine position (Moore, 2008). Later work in 1812 by McTarnan highlighted the death of a marine from the supposed “wind” without noticeable injury (Dickson, 1943). Although McTarnan’s description provides evidence in line with what is currently known about blast injury, at the time his work sparked considerable controversy and early efforts to define TBI were delayed due to the lack of overt wounds (Rosenfeld *et al.*, 2013, Moore, 2008).

Sir FW Motts, a physician in the British army during World War I, is credited as one of the first to report on the effects of blast injury on the central nervous system (Mott, 1916). His report revealed concussions were sustained from aerial compression based on post mortem examinations of soldiers (Moore, 2008). Despite the clarity of Motts’ work, his findings were disputed by Denny-Brown, a neurologist, who believed the deaths were due instead to carbon monoxide poisoning (Denny-Brown, 1945). Following work from Mott and Denny-Brown, a number of terms (shell shock, soldier’s heart, and neuropsychiatric postconcussion syndrome) were used to describe ailments quite similar to what we now recognize as TBI (Jones, 2006, Jones *et al.*, 2007).

It wasn’t until work by Fulton that the connection between concussions and what was known as ‘neuropsychiatric postconcussion syndrome’ was made (Moore, 2008). In his 1942 report, Fulton explained that death from primary blast is a true clinical phenomenon (Fulton, 1942). But even after the realization of TBI as a health concern, broad acceptance of this finding was delayed due to early reports attributing TBI symptoms to neuroses and excuses to avoid deployment, discouraging those affected from seeking proper medical care (Jones et al., 2007, Buck, 2011). Once those injured did begin to seek help, the sheer number of people requiring medical attention overwhelmed physicians such that the range of symptoms was not properly addressed (Jones, 2006). Furthermore, government intervention put pressure on many physicians to suppress attention regarding the magnitude of the problem (Jones, 2006).

Recent wars and uprisings raging in the Middle East (in Iraq Operation Iraqi Freedom and Afghanistan's Operation Enduring Freedom) have seen the reemergence of TBI as an important public health concern (Moore, 2008, Goodrich *et al.*, 2013). No longer are injuries isolated to the battlefield for terrorist acts on civilians have significantly increased since 2001 (Wolf *et al.*, 2009). Additionally, the rise in industrial and recreational accidents such as those involving vehicular and sports related injuries are confronting a health-care system previously spared from managing such injuries in their day to day practice (Wolf et al., 2009).

Physics of blast related TBI

Fundamentally a blast wave is defined by pressure over time. Blast related explosions result from chemical reactions in which a solid or liquid is rapidly converted into a gas releasing extremely large amounts of energy (Stuhmiller, 1997, Wolf et al., 2009). The rapid expansion of gas molecules following explosions compresses the surrounding air and the resulting shock wave (commonly referred to as blast wave) propagates in all directions (DePalma *et al.*, 2005, Stuhmiller, 1997). An increase in pressure due to blasts is known as blast overpressure, and it depends on: the energy from the explosion, distance from detonation, and time following blast (Stuhmiller, 1997).

Figure 1-1 provides graphical representation of common types of blast signatures: the classic Friedlander wave (representing an ideal wave with the traditional positive and negative phases) and a complex waveform, the latter of which most closely mimics realistic wave forms as the peaks and troughs are representative of blast waves encountering surfaces to transmit and/or reflect energy (Morganti-Kossmann *et al.*, 2010).

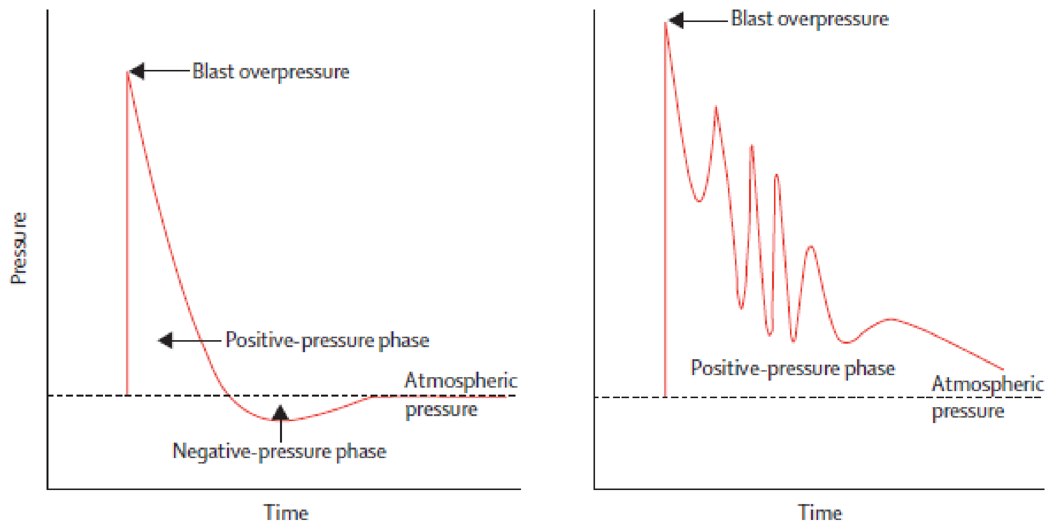

Figure 1-1. Pressure versus time curves for two types of signature blasts. Left The ideal blast wave, commonly referred to as a Friedlander curve shows an increase in pressure during the positive pressure phase until a maximal pressure (blast overpressure) is achieved followed by the negative pressure phase representing the drop in atmospheric pressure creating a partial vacuum until a return to atmospheric pressure. **Right** A complex wave form contains the same elements of a simple ideal wave with the exception of multiple peak pressures during the positive pressure phase due to interactions with surrounding structures and objects. Figure modified from Wolf et al., 2009.

Blast waves have two components: a high pressure shock wave and a blast wind (DePalma et al., 2005). The maximum pressure is known as the peak (or blast) overpressure (Figure 1-1). Injury from the actual blast wave striking living organisms is defined as primary blast injury (Mayorga, 1997). It is this pressure that is responsible for the injuries that result (Wolf et al., 2009). Pressures as high as 500 kPa have been reported to result in lethality whereas pressures as low as 20kPa may not cause injury (Wolf et al., 2009). Secondary injury results from materials such as glass, debris and surrounding structures mobilized from the blast wave striking the body (Ritenour & Baskin, 2008). As the blast wave strikes it compresses the body transferring energy to the surface. Previously it was believed that the only body structures vulnerable to primary blast injury were the auditory, respiratory, and gastrointestinal tracts (Stuhmiller, 1997). However, later work provided evidence that the nervous system is affected (Cernak & Noble-Haeusslein, 2010, Cernak et al., 1999).

Comparison of blast overpressure with ambient pressure defines the strength of a blast (Morganti-Kossmann et al., 2010). The portion of the blast wave propagating into the surrounding (undisturbed) ambient air is the blast front. As gases from explosions expand in all directions a high pressure region is produced. As air molecules are compressed forward into the blast front—away from the source of the blast-- negative pressure from the decompressed air forms behind creating a vacuum that reverses the direction of gas flow to fill the void (Figure 1-1) (Stuhmiller, 1997).

Blast waves can be measured in real-time using a piezoelctronic (or piezo-resistive) pressure transducer that generates pressure waveforms (graphical representations of changes in pressure over time) tailored to the complexity of the blast.

Blasts that occur outdoors in a free field generate a classic Friedlander waveform (Figure 1-1, left) with the rapid increase to peak pressure, an exponential decrease, followed by a prolonged under pressure before eventually returning to ambient pressure (Moore, 2008, Morganti-Kossmann et al., 2010). Deviations from this ideal wave occur with the introduction of variables that provide surfaces that can reflect waves (Morganti-Kossmann et al., 2010). Explosions in enclosed spaces are particularly dangerous because of the cumulative effects of reflections against objects encountered by the blast wave (Cernak et al., 1999). Interactions of blast waves with surrounding structures can increase the intensity of damage up to eightfold (Mayorga, 1997, Wolf et al., 2009). Pressure differences in the overpressure of the blast front and under pressure are most damaging (DePalma et al., 2005).

Damage sustained following TBI

Common types of damage following TBI include: contusions, lacerations, hematomas, countercoup, shearing of nerves, intracranial hypertension, hypoxia, metabolic imbalances, hydrocephalus and subarachnoid hemorrhages (Bryant, 2011). To generalize among the injury types, two common categories are focal versus diffuse brain injury (Smith, 2000). Focal brain injury describes injuries sustained from ‘contact forces’ (i.e. impact to head) resulting in contusions and hematomas, while diffuse injury may be apparent despite lack of direct impact injury to the head (Morganti-Kossmann et al., 2010).

Diffuse injury is more appropriately referred to as multifocal due to its common association with axonal and vascular injury, brain swelling, and hypoxic ischemic damage (Morganti-Kossmann et al., 2010, Smith, 2000). Of the two injury types, diffuse injury has been reported to be the most prevalent form of injury in patients (Morganti-Kossmann et al., 2010). Causative activities that result in diffuse injury include crashes and falls (Adams *et al.*, 1989). Normally, axons are resilient structures that can withstand deformations (Smith, 2000) however traumatic insults can produce shearing and stretching forces high enough to severely damage or completely disconnect axons due to loss of their natural elastic properties (Smith, 2000). Such insults often appear as swellings along processes that can become evident within seconds following trauma and may persist for months depending on the model (Pierce *et al.*, 1998). Consequences of such damage involve impairments to axonal transport and ion balances due to perturbations to various channels and perforations in the plasma membrane (Smith, 2000). Ultimately diffuse injury results in either reparative or degenerative mechanisms (Smith *et al.*, 2013) . Conclusive knowledge regarding which mechanism ultimately prevails has yet to be established. However, the severity of initial insult, repeated trauma and persistent swelling are indicative of degeneration (Smith, 2000). Most microscopic injuries resulting from TBI are difficult to diagnose as current imaging resources are unable to fully detect the extent of axonal damage however diffusion tensor imaging has shown promise in the ability to accurately assess axonal damage (Benson *et al.*, 2007).

Diagnosing TBI

The Glasgow coma scale (GCS), established in 1974, is one of the most prominent neurological scales used to diagnose the extent of TBI (Grote *et al.*, 2011). Scores assessed from three areas (eye opening, verbal and motor responses) are combined and used to classify damage as mild, moderate or severe in conjunction with clinical observations, and diagnostic imaging (Kim & Gean, 2011). Symptoms of mild TBI include: confusion, disorientation, loss of conscious for 30 minutes or less, a GCS of 13-15, and post-traumatic amnesia durations not greater than 24 hours (Ruff *et al.*, 2009). Specificity of mild TBI diagnosis is poor due to ambiguous symptoms ranging from headaches, cognitive dysfunction, attention difficulty and imbalance (Rosenfeld et al., 2013). Moderate TBI can encompass some of the same features of mild TBI with exceptions involving loss of consciousness ranging from 30 minutes to 24 hours, and post-traumatic amnesia lasting from one to seven days (Bryant, 2011). Extensions in loss of consciousness and amnesic durations beyond moderate TBI as well as significant cognitive deficits are seen in severe TBI (Glaesser *et al.*, 2004).

The challenge in accurately diagnosing TBI is due to the ambiguity of its psychological symptoms. For example, severe forms of TBI are sometimes confused with post traumatic stress disorder (PTSD) (Bryant, 2011, Kamnaksh *et al.*, 2011). PTSD is an anxiety disorder commonly diagnosed one month following trauma if specific criteria are met (1. witnessing an event that threatens safety, 2. continually re-experiencing the traumatic event, 3. active avoidance behaviors and inability to recall 4. significant behavioral changes such as: irritability, insomnia, overstimulation) (Bryant, 2011). The overlap in TBI and PTSD is due to cases of TBI involving similar emotional dissociation such as decreased awareness of one's surroundings and amnesia (Glaesser et al., 2004).

Diagnostic imaging is used to determine type and extent of cellular injury (Kim & Gean, 2011, NIH-NINDS, 2013). Ease of use and accuracy has made noncontrast computed tomography (CT) scans the diagnostic of choice in acute settings because it can distinguish between extra-axial (e.g. epidural, subdural) and intra-axial (contusion, hematoma, traumatic axonal injury) hemorrhages (Kim & Gean, 2011). Although CT scans provide valuable insight, they are limited in the ability to detect physiological impairments that result from secondary cascades such as cerebral perfusion, blood flow and changes in oxygen (Kim & Gean, 2011).

When compared to CT scans magnet resonance imaging (MRIs), specifically diffusion tensor imaging (DTI), offers greater sensitivity in diagnosing damage beyond hemorrhages and contusions (Kim & Gean, 2011, Alsop *et al.*, 1996). What has made DTI especially helpful in diagnostics is its ability to map microstructural brain information on axon orientation (Wintermark *et al.*, 2004). Results from DTIs correlate well with severity of cognitive impairments.

Current therapies following diagnosis include stabilizing patients to avoid additional injury and preventative measures. This is achieved by monitoring blood pressure and maintaining brain oxygen levels following acute diagnosis. Long term care focuses on rehabilitative, physical, and speech therapies. (NIH-NINDS, 2013).

Animal models used to study TBI

Several models have been developed to help elucidate mechanisms that cause damage. Early efforts to understand TBI focused on the mechanics of primary injury through *in vitro* models. More recently the majority of studies have centered on rodents as the animal of choice due to costs and ability to standardize outcomes (Xiong et al., 2013). Similarity of cell and molecular events makes rodents a popular choice to model TBI (Morganti-Kossmann et al., 2010). However, the ideal animal model does not exist. Part of this limitation is due to the fact that the majority of models currently available result in focal or diffuse injury whereas clinical cases are often a combination of both (Morales et al., 2005). Furthermore, it is difficult to account for complexities of pre-existing conditions, medical treatment and additional insults such as hypertension, hypoxia and ischemia.

Use of animal models to understand TBI gained momentum in the early 80's. Initial work involved use of a variety of species (cats, dogs, and non-human primates) (Xiong et al., 2013). A decade later use of small animals began to dominate the field. Given their low cost and well characterized genetics, small animals remain the most popular choice to model TBI today. However, it has been reported that differences in strains of the same species results in differences in cognition and molecular responses. In addition, although the appeal of genetic manipulation offers valuable insight (Longhi *et al.*, 2001), data from genetically modified rodents may add to the variation (Morganti-Kossmann et al., 2010).

The challenge that persists in TBI is that no one case is identical. Variations in regions affected, severity and type of injury as damage often results from the combined effects of primary, secondary and tertiary blast injury (Morales et al., 2005, Mayorga, 1997). Five models (weight drop, fluid percussion injury (FPI), cortical controlled impact (CCI), penetrating ballistic-like brain injury (PBBI), and blast injury) each with the ability mimic a specific type of TBI and its severity have been used (Morales et al., 2005) and will be briefly discussed.

WEIGHT DROP

Feeney *et al.'*s weight drop model is often credited as the original TBI model (Morales et al., 2005). First developed in 1981, Feeney's model uses a weight dropped onto exposed dura following a craniotomy to cause cortical contusion (Feeney *et al.*, 1981). Within three hours following injury hemorrhages in white matter are observed, necrosis by twenty-four hours, and expanding cavitations within two weeks (Xiong et al., 2013). Impairments with this model have been reported beyond three months following trauma. Following Feeney *et al.*'s model, Shohami *et al.* in the late 1980's established a weight drop model to simulate closed head injury (Xiong et al., 2013, Shohami *et al.*, 1988). A weight dropped onto one side of an unprotected rodent skull positioned on top of a hard surface recapitulated blunt focal injury. Impairments in neurobehavior, activation of microglia and astrocytes as well as neurodegeneration make this model useful in evaluating clinical conditions (Foda & Marmarou, 1994). However, one drawback is the lack of reproducibility (Xiong et al., 2013).

Developed in the mid-90's Marmarou *et al.*'s weight drop model is more of an impact-acceleration model (Marmarou *et al.*, 1994). It is used to evaluate diffuse TBI that results from falls or vehicular accidents. The trauma is produced from brass weights allowed to freely fall from specific heights. The exposed animal skull is affixed with a disc made of stainless steel to prevent fracture. Widespread neuronal damage (notably in the corpus callosum, optic tracts and brainstem), motor damage and cognitive impairments have been observed (Xiong et al., 2013). Drawbacks to this model, and the premise of weight drop as a whole, are variability and high mortality rates.

FLUID PERCUSSION INJURY

Trauma is sustained from a pendulum striking a fluid filled piston reservoir attached to a craniotomy in the skull (O'Connor *et al.*, 2011). The pulse of pressure generated from the piston deforms the exposed dura, either centrally around the midline or laterally over the parietal bone, between bregma and lambda (Cernak, 2005). Severity of injury is dependent on the strength of the pressure pulse generated (Dixon *et al.*, 1987). FPI models have been employed to mimic intracranial hemorrhage, swelling and damage to grey matter (Xiong et al., 2013).

CONTROLLED CORTICAL IMPACT

First characterized in ferrets, this model involves an impact apparatus (pneumatic or electromagnetic) forcing a rigid impactor onto intact dura resulting in cranial deformation (Morales et al., 2005, Xiong et al., 2013). The widespread deformation is seen in the cortex, hippocampus and thalamus (Xiong et al., 2013). This model has been shown to result in cortical tissue loss, subdural hematomas, concussion and axonal injury (Lighthall *et al.*, 1990). Severity of injury is based on the velocity of impact, degree of cortical deformation and tissue loss. Although injury is reproducible, cost and complexity of operation have posed a challenge (Xiong et al., 2013).

PENETRATING BALLISTIC-LIKE BRAIN INJURY

Originally developed as a penetrating missile model to deliver trauma in cats, the ballistic brain injury of PBBI is relevant for moderate to severe trauma (Carey *et al.*, 1989). Use of high energy projectiles such as a metal rod or expanding elastic balloon creates a cavity in the brain tissue. The utility of this model is its applicability to projectile injury, such as shrapnel, and gunshot wounds. Trauma that results includes: white/grey matter damage, brain swelling, seizures and inflammation (Xiong et al., 2013). A major setback is the need for standardization.

BLAST INDUCED NEUROTRAUMA

In blast models of TBI animals are exposed to blasts via pressures from shock tubes or detonation of explosives whose quantities are known (Svetlov *et al.*, 2009). Severity of injury depends on the following: open versus closed environments (the latter of which results in the most damaging injury), energy of the blast, distance from blast and position, and presence of protective wear (Rosenfeld et al., 2013, Kuehn *et al.*, 2011, Svetlov et al., 2009). Additional factors such as the number of blast exposures as well as intervals between exposures significantly contribute to injury outcome and susceptibility (Rosenfeld et al., 2013). When the blast wave encounters biological tissue, shear and transverse wave formation cause stresses that can produce different pathological effects on brain structures, especially white matter tracts (Moore, 2008).

It is worth noting that blast induced TBI (bTBI) is traditionally divided into four phases—primary, secondary, tertiary and quaternary—that are indicative of the mode of trauma (Morganti-Kossmann et al., 2010, Burgess *et al.*, 2010). Primary bTBI occurs at the time of trauma and is caused by the propagation of the blast wave (Morganti-

Kossmann et al., 2010, Rosenfeld et al., 2013). It is this TBI model that most appropriately mimics injuries sustained in combat (Cernak et al., 1999). All forms of bTBI (mild moderate and severe) may be encompassed by primary damage, whereas the remaining phases of TBI are commonly associated with moderate and severe TBI (Rosenfeld et al., 2013). Secondary injury is due to cranial impact of projectiles which have been set in motion by the blast wave (Stuhmiller, 1997). Secondary damage is usually associated with ongoing neurodegeneration, cell death and additional symptoms are defined as secondary damage (Rosenfeld et al., 2013, Morganti-Kossmann et al., 2010). Blast induced collisions of the injuree with nearby objects and structures results in tertiary injury, whereas quaternary trauma is caused by injury from chemicals or gases from the surrounding blast environment (Mayorga, 1997).

Overall goals of my preliminary research

As previously stated, no one model can adequately recapitulate the broad range of processes experienced in a clinical setting. However, given the rise of TBI cases reported in the military, my research has focused on the blast induced trauma model because it most closely mimics the trauma many soldiers and civilians experience on the battlefield. To assess the extent of damage, my preliminary research will target three specific brain regions: the dentate gyrus of the hippocampus, the RSC, and the visual cortex. Potential cellular responses throughout these regions include: activation of astrocytes, modulation of calcium-binding proteins, and changes in levels of neurogenesis in the dentate gyrus. One essential factor of my research is identifying the time point following blast injury that results in the clearest evidence of damage. The majority of TBI studies typically have employed invasive models such as a CCI and FPI which routinely require anesthesia. Because anesthesia could be a major confound I also want to determine what impact different combinations of anesthetics have on bTBI.

Rationale for the brain regions to be studied

Three of the most prevalent symptoms sufferers of TBI face are impairments in: memory, cognition and vision (Yu *et al.*, 2008, Cockerham *et al.*, 2009, Pandit *et al.*, 2013). Therefore I chose to examine brain regions associated with each one of these impairments as follows: memory, dentate gyrus; cognition, RSC; and vision, visual cortex.

<u>Dentate Gyrus</u>

The dentate gyrus is a three layer structure within the hippocampus, a region involved in learning and memory (Figure 1-2). At its center is the hilus, also known as the polymorphic zone owning partially to the a variety of cell types such as mossy cells and fusiform cells present (Scharfman & Myers, 2012). The principal layer enclosing the hilus is the granule cell layer. Granule cells are the predominate cell type within the granule cell layer. However other populations of neurons, like the pyramidal basket cells located near the border of the granule cell layer and hilus, exist (Amaral *et al.*, 2007). The outermost layer of the dentate gyrus is the molecular layer. This relatively cell free layer mainly contains dendrites from the granule cells (Figure 1-2 E).

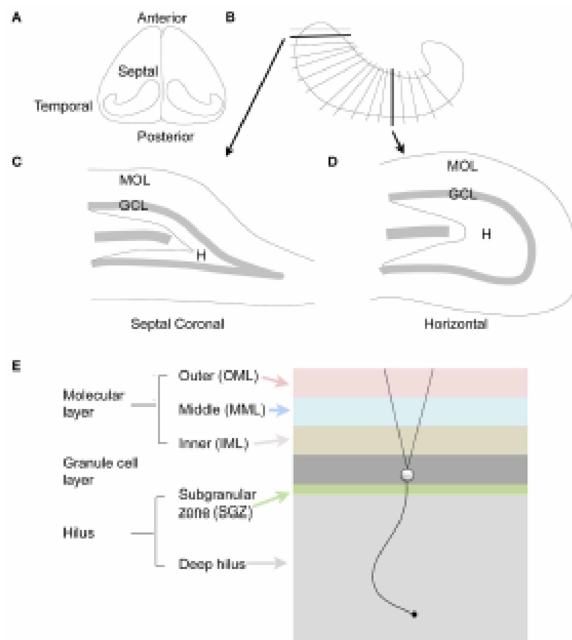

Figure 1-2. Anatomy of the rodent dentate gyrus. A. Dorsal view indicating location of hippocampi **B.** Overall shape with examples of plane of sections that can be obtained **C.** Coronal section from the septal region. **D.** Horizontal section. **E.** Organization of layers within the dentate gyrus. A single granule cell is depicted to show orientation of dendrites into the molecular layer and an axon into the hilus. Figure obtained from Scharfman & Myers, 2012.

The dentate gyrus is believed to underlie many pathological effects of TBI as alterations to memory remain one of the most prevalent symptoms of TBI (Bonislawski et al., 2007, Dash *et al.*, 2001). The vulnerability of the dentate gyrus to trauma is due, in part, to its role as a filter against propagation of aberrant activity to higher brain regions (Bonislawski et al., 2007). Work by Gao *et al.* (2008) showed that the highest number of degenerating neurons were in the dentate gyrus following moderate CCI induced TBI, whereas no degeneration was seen in CA1 or CA3. Of the degenerating neurons in Gao *et al.*'s study, 80% were found in the inner granule cell layer. Further analysis identified that the cells affected were newborn immature neurons. It is thought that targeted vulnerability of immature dentate gyrus neurons could be involved in learning and memory impairments following TBI (Vakil, 2005). Newborn granule neurons are continuously produced and integrated into the established hippocampal network responsible for consolidation of new memories and learned behaviors (Kempermann & Gage, 2000). Thus death of these newborn neurons following TBI could have a key role in the learning and memory deficits associated with TBI (Gao *et al.*, 2008).

In the dentate gyrus neural stem cells in the subgranular zone (SGZ) transition into newborn immature neurons that migrate to the SGZ and eventually reside in the inner one-third of the granule cell layer (Gao et al., 2008). Each cell type in the dentate gyrus possesses a unique function. The level of vulnerability across different cell types has not yet been established (Lowenstein *et al.*, 1992). Much of the difficulty is due to variations in damage with injury severity, age, and the TBI model used (Markgraf *et al.*, 2001). Understanding the distribution of cell vulnerability and death would provide valuable information. Furthermore, investigations into cell-type specificity following TBI can provide clear insight into potential therapeutics (Gao et al., 2008).

Retrosplenial Cortex

My choice to focus on the RSC was due solely to its anatomical position. I hypothesized that because the RSC is the brain regions directly below where the blast is administered it would experience damaging effects from blast injury. Figure 1-3 shows a general schematic of the location of the RSC across a single coronal section.

The RSC is part of the posterior cingulate cortex (Broadmann areas 29 and 30) and is located above the corpus callosum between the hippocampal formation. The full details regarding extensive connections to and from the RSC are outside the scope of this master's thesis. However three of the main connection pathways from the RSC include the hippocampal formation, the parahippocampal region and thalamic nuclei (Wyss & Van Groen, 1992). Behavioral lesion studies provide evidence of the RSC contributing to navigation, learning, and memory, specifically episodic memory (Vann *et al.*, 2009, Parron & Save, 2004). In addition to behavioral paradigms the RSC has been explored in trauma and neurodegenerative diseases. For example a study examining 27 patients with TBI found significant atrophy in the posterior cingulate gyrus that correlated with injury severity (Yount *et al.*, 2002). Because of its complicated structure, extensive connections and innervations to and from a large number of brain regions (Vann et al., 2009) exploring disturbances in this region could provide additional insight into the relationship between the role of damage in the RSC following TBI.

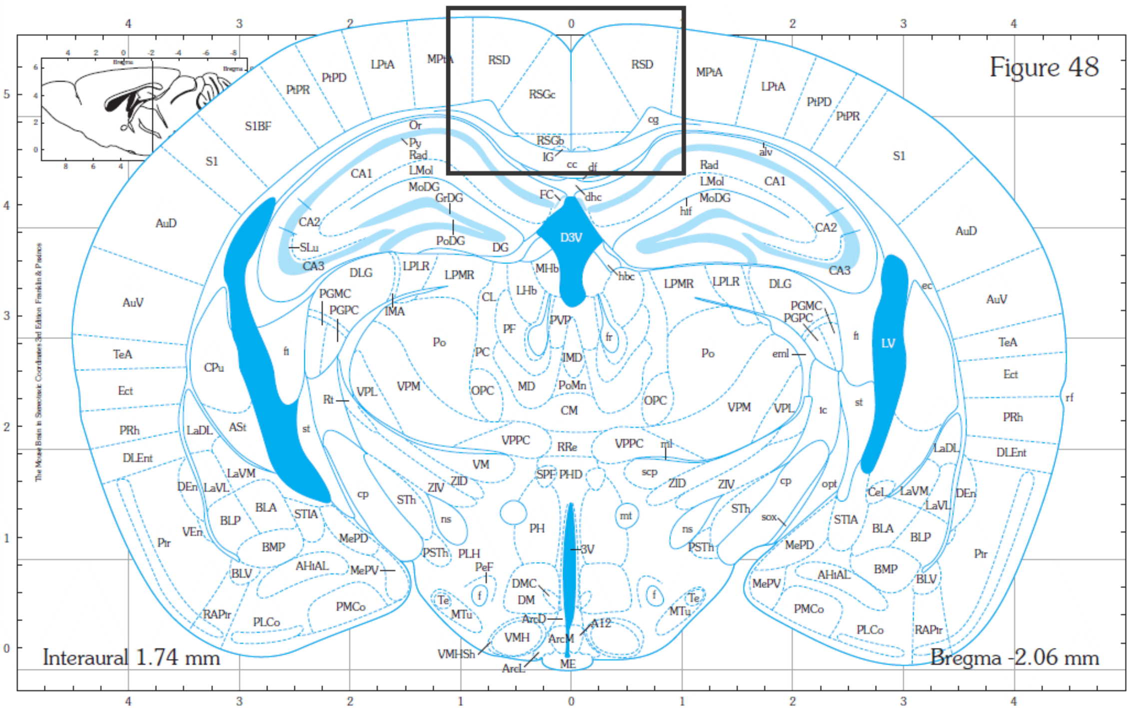

Figure 1-3. Location of RSC across a single coronal section of the rodent brain.

Adapted from The Mouse Brain Atlas 3rd Edition (Franklin & Paxinos, 2008).

Visual Cortex

Up to 85% of individuals affected with TBI report problems with vision (Kapoor & Ciuffreda, 2002). Common vision disorders following head trauma include accommodation, version deficits (e.g. saccades), visual field deficits and photo sensitivity (Cockerham et al., 2009). Given the range of visual deficits common in bTBI it is possible that the visual system is affected at multiple levels. Fortunately, the high level of organization within the visual cortex (Figure 1-4) lends itself well to TBI investigations (Cheng & Povlishock, 1988).

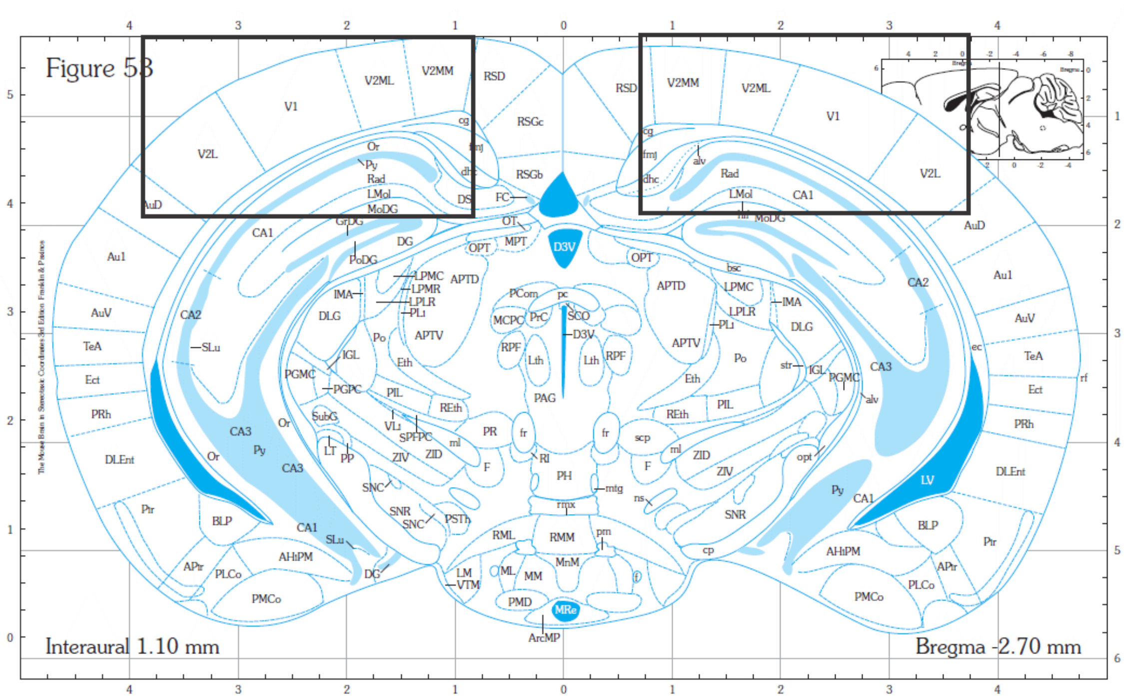

Figure 1-4. Location of the visual cortex across a single coronal section of the rodent brain. Adapted from The Mouse Brain Atlas 3rd Edition (Franklin & Paxinos, 2008).

Rationale for the cellular markers used

Immunocytochemical markers were chosen to visualize changes in specific populations of interneurons, neurogenesis, or astrogliosis to assess effects of bTBI.

Elevation of Calcium following TBI

Calcium ions have been shown to play a key role in virtually every cellular process from cell proliferation to synaptic transmission (Bootman & Berridge, 1995, Miller, 1991, Berridge, 1998). The essential nature of calcium requires that its intra- and extracellular concentrations be carefully regulated. A variety of mechanisms involving ion channels and pumps on the plasma membrane and organelles are employed to ensure that the intracellular concentration (approximately 100nM) remains much lower than the extracellular concentration (approximately 1mM) (Weber, 2012, Miller, 1991).

Excitoxicity is a phenomenon that can result when the delicate balance required for calcium homeostasis in neurons is disrupted causing the intracellular concentration of calcium to be high enough to initiate a number of detrimental secondary cascades that can end with cell death (Weber, 2012). Even in the absence of cell death alterations of calcium homeostasis in surviving neurons have been reported to contribute to cognitive deficits (Deshpande *et al.*, 2008). Elevation in calcium levels following TBI are attributed to physical deformation of the plasma membrane providing a direct mode of entry for calcium, as well as alterations in membrane proteins causing increases in ions like Na^+ that allow for an indirect mode of calcium entry (Weber, 2012).

Although a number of calcium stores and pumps exist within neurons to regulate calcium levels, their response time to sequester calcium can be slow (Miller, 1991). An important mechanism used to regulate fast influxes of calcium involves calcium-binding proteins (CBPs). Their high affinity for calcium (10^{-3} -10^{-8} M) allows these soluble cytoplasmic proteins to act as buffers (Miller, 1991). A number of CBPs with differing kinetic properties have been identified in diverse neuronal populations (Baimbridge *et al.*, 1992). It has been proposed that cellular vulnerability to elevation of intracellular calcium differs with each CBP (Isaacs *et al.*, 2000). Work from Freund et al. in 1990 showed that calbindin positive cells in hippocampi (specifically CA1) of rats were not as sensitive to ischemia as parvalbumin containing containing cells. It is believed that cells containing certain CBPs may be more resistant to injury due to increased buffering, while others may be more vulnerable because of the high uptake and release (Freund *et al.*, 1990). In the present study calretinin and parvalbumin were selected because of their dual ability to function as both calcium buffers and as anatomical markers for non-overlapping interneuron populations (Schwaller, 2009, Andressen *et al.*, 1993).

<u>Changes in Neurogenesis</u>

Neurogenesis in the subgranular zone of the dentate gyrus occurs throughout adulthood in the brains of mice, rats, human and non-human primates (Zheng *et al.*, 2013). Newly generated cells are able to differentiate into granule cells that can integrate within established networks (Zheng et al., 2013, Urrea *et al.*, 2007). Evidence of this was most convincing in a study by Emery et al. (2005) that showed newly generated granule cells were capable of extending their projections along the mossy fiber pathway into CA3. Numerous studies have reported increases in neurogenesis following trauma (Curtis *et al.*, 2003, Jin *et al.*, 2004, Jin *et al.*, 2006, Sgubin *et al.*, 2007). For example, trauma models involving ischemia have shown increases in neurogenesis following injury (Zheng et al., 2013). Although functionality of the increased neurogenesis occurring following trauma has yet to be fully established, there is great interest in the possibility of repairing damaged circuits. In the present work doublecortin, a microtubule associated protein expressed in neuronal precursors, was used to visualize changes in neurogenesis following bTBI.

Occurrence of Astrogliosis

Astrocytes are one of the major glial cell types in the central nervous system (CNS) (Brahmachari *et al.*, 2006). Functionally astrocytes play important roles in maintaining the integrity of the blood brain barrier, protection against neurotransmitter excitotoxicity, promotion of synaptic plasticity, and coordination of neuronal activity via gap junctions (Middeldorp & Hol, 2011). Upon injury, astrocytes become activated and undergo morphological and functional changes (Torre *et al.*, 1993). Marked hypertrophy of soma and processes are hallmarks of astrocytic response to injury.

Although activated astrocytes have been shown to play an important role in restorative processes by regulating ions in extracellular space, the response of astrocytes following TBI has also been implicated in its pathology due to their involvement in inflammation (Brahmachari et al., 2006, Stringer, 1996). Persistent astrocytic inflammation can result in neuronal death and brain injury due to the production and secretion of neurotoxic substances (Brahmachari et al., 2006). A hallmark of astrocytic activation is elevation in levels of glial fibrillary acidic protein (GFAP) that correlates with severity of astrogliosis (Amaducci *et al.*, 1981). GFAP is the main intermediate filament protein within mature astrocytes that is responsible for its changes in morphology and movement (Middeldorp & Hol, 2011, Brahmachari et al., 2006). Injury in the CNS, particularly mechanical injury increases GFAP expression that can ultimately result in formation of glial scars (Middeldorp & Hol, 2011). Identification of astrogliosis has been reported minutes to hours following trauma (Sword *et al.*, 2013). While Kim et al. (2012) showed astrogliosis to persist up to 15 days following cryogenic TBI (use of a cold metal probe to produce focal injury upon contact with the skull's surface). Because the astrocytic response has been reported to differ with type, severity and duration of brain injury my goal was to assess whether astrogliosis occurs during acute recovery (48 hours through two weeks) of blast-induced trauma.

Determining key time point(s) following injury

Work identifying the types of injuries sustained from TBI models has provided helpful bridges to the clinical realm. As previously stated, some damaging effects have been observed moments after primary insult (Sword et al., 2013) and can persist months following trauma (Cheng & Povlishock, 1988). Understanding the initiation and duration of injury cascades would greatly benefit efforts in the creation of pharmacological therapies to eventually prevent or treat TBI. A number of studies have used the same recovery windows as the present study (Urrea et al., 2007, Kernie & Parent, 2010, Matthews *et al.*, 1998). However, the vast majority of studies employed invasive TBI models and they assessed behavioral rather than cellular or anatomical outcomes. Thus my preliminary work offers valuable new information. The analysis of specific cellular or anatomical responses to bTBI has the benefit that it might provide insight into potential prophylactic therapies needed to prevent or ameliorate injury or to restore functionality to damaged cortical and hippocampal circuits affected in this type of trauma.

Possible influence of anesthesia

Ethical considerations have resulted in all animal models of TBI to date using anesthetics to minimize pain whenever possible. However, emerging evidence indicates that the choice and overall presence of anesthetic can significantly affect severity of results (Rowe *et al.*, 2013, Statler *et al.*, 2006). In particular, inhalational and injectable anesthetics offer a certain degree of neuroprotection which varies with anesthetic type, duration of exposure, and experimental model (Schifilliti *et al.*, 2010). Common agents such as isofluorane and ketamine show a dose dependent and exposure-time dependent neuro-protective effect (Schifilliti et al., 2010).

The popularity of invasive TBI models (e.g. FPI and CCI) have added to the challenge of clearly identifying the influence of anesthetics. The craniotomies performed require large anesthetic dosages over long durations and the animals have to recover from the procedure prior to the trauma which adds to the cellular complexity. For example, sham animals have been reported to suffer from spontaneous seizures and other histopathologies that are seen after trauma (Carbonell & Grady, 1999). Moreover, there are differences in outcomes in studies using mice versus rats (Carbonell & Grady, 1999). Given the need for trauma models more analogous to actual damage sustained in combat, a major goal of my preliminary work is to investigate the effects of the commonly used anesthetics ketamine and xylazine as well as the analgesic buprenorphine in bTBI.

Chapter 2

MATERIALS AND METHODS

Cranium Only Blast Injury Apparatus

Construction of the cranium only blast injury apparatus (COBIA) was based on the blast injury model established by Kuehn et al. (2011). The essential component of the COBIA was a .22 caliber single-shot, powder-actuated tool (Ramset RS22; ITW Ramset, Glendale Heights, IL) that delivers the blast. The tool was modified by removal of the piston that normally drives the fastener. Once modified it functioned like a firearm that permits undampened propagation of the blast wave through the barrel. Crimped brass cartridges were used to deliver blasts (power hammer loads power level 4, yellow color coding with 179 +/- 5mg smokeless powder). A custom fabricated stand holds the firearm vertically so that the blast wave is directed downward into a blast dissipation chamber (BDC) made of polyvinyl chloride (PVC) piping that is firmly fitted to the muzzle of the firearm (Figure 2-1A). A circular opening at the end of the PVC pipe holds the head of the mouse in place at the BDC-cranium interface (BDCCI) (Figure 2-1B and C).

Blast Wave Measurements and Calibration

A precision dynamic high frequency piezoelectric pressure transducer (Model: 113B21 High Frequency ICP® pressure sensor, PCB Piezotronics, Inc., Depew, New York) was used to record blast waves produced by the COBIA. The sensor is positioned where the head of the mouse would be inside the apparatus. A constant current supply (Model 5421, Columbia Research Laboratories, Inc., Woodlyn, PA) provides power to the transducer. Outputs were digitized using an A to D converter (Analog Devices, ADAS3022) before saving waveforms for offline analysis.

To determine the greatest non-lethal blast overpressure, three different power loads (power hammer loads power levels 2, 3, and 4 with-brown, green, and yellow color coding respectively) were analyzed over varying lengths (9.8 and 16.0 cm) of PVC pipes. The different lengths of PVC pipes and diameters did not produce a noticeable difference in blast overpressure (data not shown). However, pressures generated differed for each cartridge load with the yellow power load producing the greatest non-lethal pressure (an average of 534 kPa) (Figure 2-2).

Blast Injury Procedure

All procedures were approved by the Institutional Animal Care and Use Committee at Boston University. C57BL/6 mice (6-12 weeks) were purchased from Charles River Laboratories or kindly provided by the laboratory of Dr. Ian Davison at Boston University. Mice were acclimated for one week in the Laboratory Animal Care Facility on Boston University’s Charles River Campus.

In some studies the adult mice (n=2) were anesthetized at least 10 minutes prior to blast with ketamine (75 mg/kg, IP) and xylazine (13 mg/kg, IP). Prior to blast a circular spot Band-Aid was placed at the top of the head for protection from gun powder. Mice were placed into the opening of the PVC pipe in a prone position until one third of the occipital crest was visible in the inner circumference of the BDCCI (Figure 2-1C). Loosely packed cotton was placed under the head to position it optimally and to allow maximal downward acceleration of the head immediately following blast. If respiration did not resume following blast trauma chest massages were performed until recovery or cardiac arrest was determined. Sham mice (n=3) underwent the same procedures as experimental groups with the exception of exposure to blast trauma. All animals recovered in cages heated with a 37° C heating pad to facilitate adequate thermoregulation. Once recovery of full mobility was noted a single subcutaneous injection of 0.1-0.2 mg/kg buprenophrine was administered.

Pilot Blast Injury Study

A pilot study was performed to assess the neuroprotective role of ketamine which is known to block NMDA receptors (Rowe et al., 2013). One group of mice (n=2) was sedated using ketamine (75 mg/kg, IP) and xylazine (13 mg/kg, IP) thirty minutes prior to blast, while a second group (n=2) received only xylazine (13 mg/kg, IP) thirty minutes prior to blast. Both groups received buprenorphine (0.1 mg/kg, SC) subsequent to the blast. All mice in the pilot study were restrained during the blast using a cylindrical mouse restrainer (Stoelting Co. Wood Dale, IL). Blast exposure and recovery were carried out as explained above.

Tissue Preparation

Following specified recovery intervals mice were heavily anesthetized with isofluorane gas. Once surgical plane of anesthesia was confirmed, the chest and abdominal cavity were quickly opened, several large cuts were made in the liver to allow outflow, and the animal was perfused through the left ventricle with 0.9% NaCl saline containing 0.4% heparin to remove the blood. Blood clearance was deemed adequate when the liver appeared yellow at which time 4% paraformaldehyde in 0.1 M phosphate buffer (PB, pH 7.4) was used to perfuse for five minutes.

Following perfusion the mice were decapitated. The brains were harvested and dissected to expose the ventricles whenever possible using an adult mouse brain slicer matrix (BSMAS001-1, Zivic Instruments, Pittsburgh, PA) prior to immersion in 4% paraformaldehyde for three hours at room temperature.

Cryoprotection

Following fixation all tissue was cryoprotected in PB containing sucrose concentrations that were gradually increased from 5% to a final solution containing 30% sucrose that was left to incubate overnight at 4˚C. Optimal cutting temperature media (Andwin Scientific Tissue-Tek CRYO-OCT Compound) was used to embed tissue before being flash frozen using dry ice. Coronal 35 µm thick brain slices were sectioned using a cryostat (Reicher-Jung) and mounted on Colorfrost Plus subbed slides (ThermoFisher Scientific, Waltham, MA). Once mounted slides were kept at -18˚C for a minimum of 24 hours, to facilitate adherence of tissue to slides, prior to immunocytochemical analysis.

Immunocytochemistry

The immunocytochemistry protocol used has been established previously (Pong *et al.*, 2007). Cryostat sectioned slides were brought to room temperature and washed in PB prior to placement in a 5% normal serum (Jackson ImmunoResearch Laboratory, Inc. West Grove, PA) that was always the same host species as secondary antibody diluted in PB-0.3% TritonX100 (PBTx) for one hour to avoid non-specific binding of secondary antisera. Following removal of blocking solution the tissue was incubated in primary antiserum (Table 1) diluted in PBTx overnight at 4˚C. Prior to incubation in appropriate fluorescently conjugated secondary antisera, slides were washed in PB. All secondary antisera were diluted 1:500 in PBTx and allowed to incubate on slides for a minimum of two hours at room temperature in a dark chamber after which slides were again washed in PB and cover slipped with glycerol (1:10 in PB, pH 8.5-9.0, Fischer Scientific) or DAPI with VectaShield (Vector Labs, Burlingame, CA).

TABLE 1. PRIMARY ANTISERA USED

Primary Antisera	Host	Dilution Used	Source
Calretinin	Rabbit	1:1000	Chemicon
Parvalbumin	Rabbit	1:5000	Novus Biologicals
Doublecortin	Goat	1:200	Santa Cruz Biotechnology
GFAP	Goat	1:500	Santa Cruz Biotechnology

Image Analysis

A Fluoview 10i confocal microscope was used for visualization. Image J analysis software (Rasband, W.S., ImageJ, U. S. National Institutes of Health, Bethesda, Maryland, USA, http://imagej.nih.gov/ij/, 1997-2012) was used to generate inverted grayscale images such that signal appeared black. Corel Draw (Ottawa, ON) was used to label and arrange the images.

Cell Counting

Confocal and Image J settings for each antibody were matched across experimental and sham groups (Figure 2-3A). Once inverted in ImageJ, the ‘threshold’ option was used to isolate labeled somata for each image (Figure 2-3B). To avoid counting background pixels, images were eroded and dilated (Figure 2-3C). A size exclusion filter was used to avoid counting noise pixels that made it through the erosion and dilation processes. The minimum area to exclude was found by measuring the area of approximately of 5-10 of the smallest somata. These values were averaged and used as the minimum value to be detected and kept by the size exclusion filter. The ‘analyze particle’ function was employed for cell counting. Masks of the somata counted were overlaid against the original image as a final way to ensure that counts performed did not contain background pixels and that the results indicated actual cells (Figure 2-3D).

The number of cells counted for sham and experimental groups were averaged within categories and entered into Microsoft Excel so that the means could be calculated and graphed.

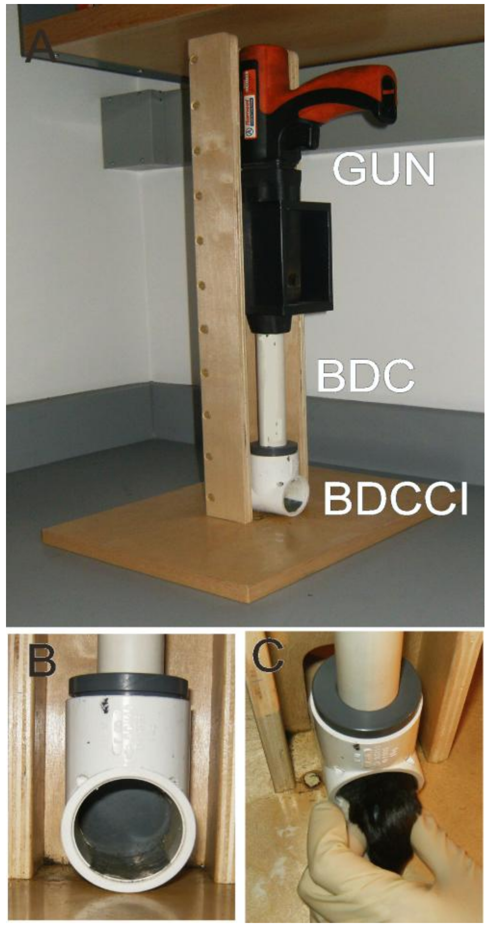

Figure 2-1. The Cranium Only Blast Injury Apparatus (COBIA). The .22 caliber firearm is positioned vertically to deliver blast into the BDC which connects with BDCCI that holds the head of the mice **(A)**. Mice are positioned in the BDCCI **(B)** and held in place to while subjected to blast **(C)**. BDC=blast dissipation chamber, BDCCI=blast dissipation chamber cranium interface.

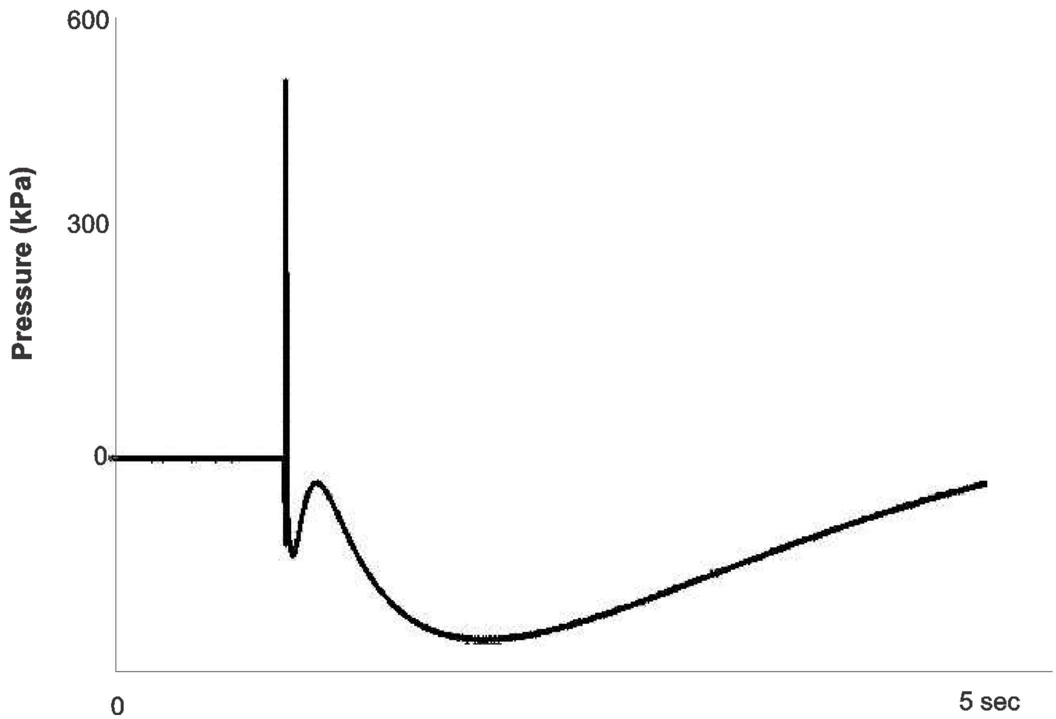

Figure 2-2. Wave form and pressure (kPa) produced by the COBIA.

Low resolution graph of the pressure wave form (averaging 534 kPa) generated from COBIA.

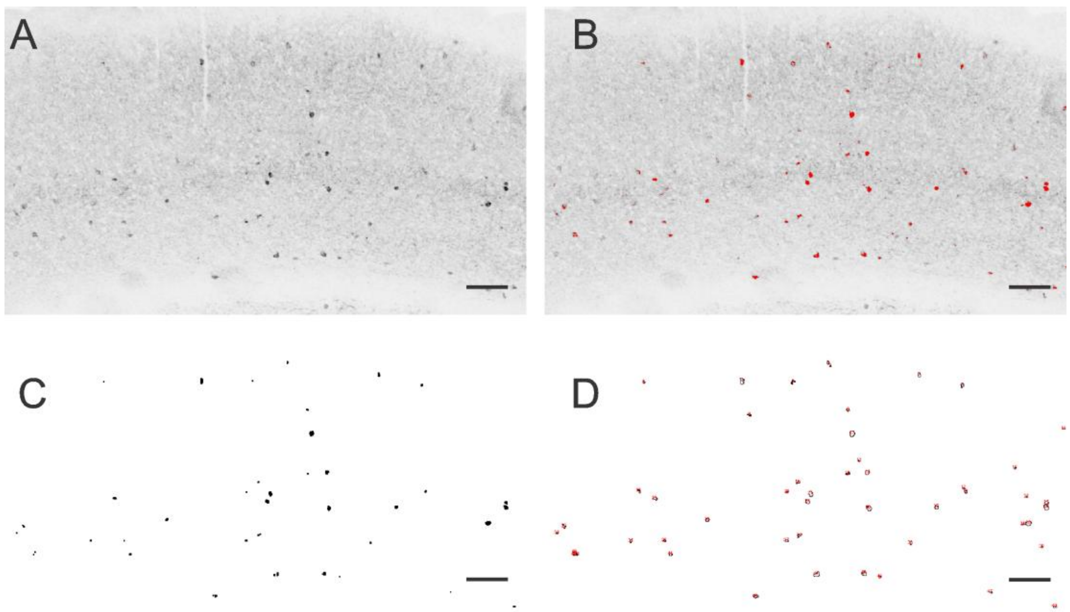

Figure 2-3. Cell Counting Analysis. A. Once settings were optimized and matched across groups images were converted from 16 to 8-bit and inverted such that signal appeared black. **B.** The ‘threshold’ option was used to isolate cells to be counted (red dots). **C.** Images were eroded to remove background noise pixels and dilated for ease of analysis. **D.** Following use of a size exclusion filter the analyze particle function counted cells. Overlays of outlines for the cells counted were reviewed as a final method to ensure accuracy of counts. Scale bars=100 microns.

Chapter 3

Response of bTBI in the dentate gyrus

Time Course Following Trauma

Immunocytochemical analysis of the calcium-binding protein calretinin allowed me to indirectly assess changes in calcium. Three specific time intervals (48 hours, one week, and two weeks) following bTBI in animals administered the anesthetics ketamine, xylazine and the analgesic buprenorphine were examined.

A prominent increase in calretinin staining was observed, particularly in the inner molecular layer, 48 hours following bTBI (Figure 3-1B) compared to sham (Figure 3-1A). In addition, a large increase in staining intensity and number of cells in the hilar region was observed 48 hours after blast trauma (Figure 3-1B). Animals that recovered for one and two weeks following blast (Figure 3-1C and D, respectively) showed a large reduction in staining of the inner molecular layer and virtually no cells were detected in the hilus compared to sham (Figure 3-1A).

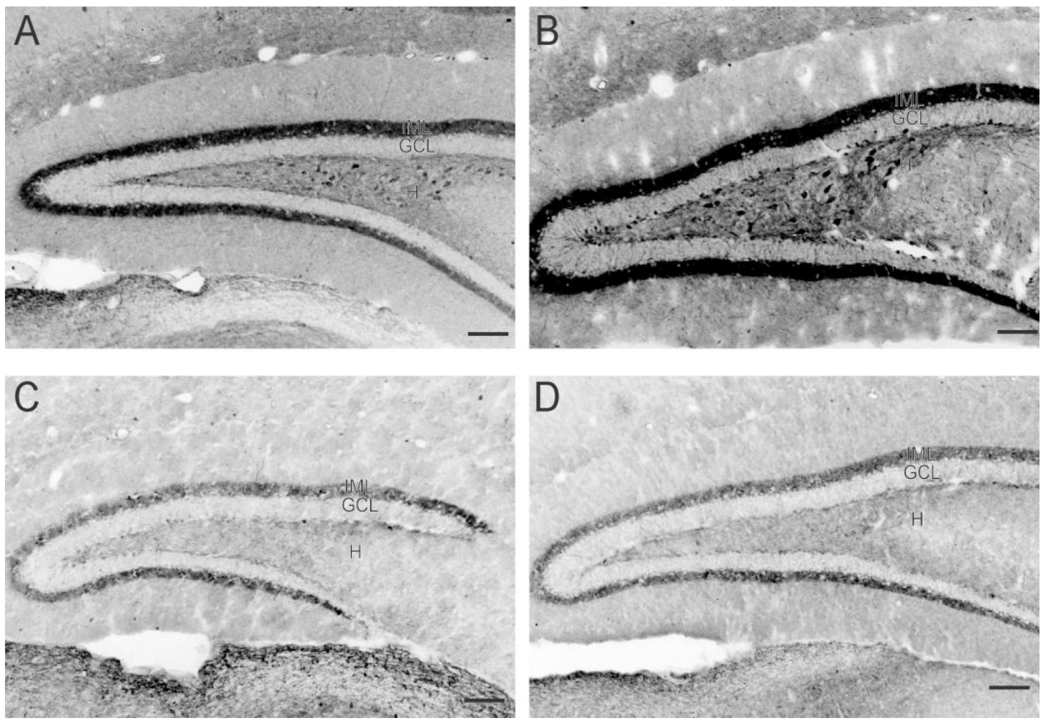

Figure 3-1. Changes in calretinin expression in the dentate gyrus following bTBI in animals anesthetized with ketamine, xylazine, and buprenorphine. Compared to sham mice **(A)** there was a large increase in the intensity of staining in the inner molecular layer and hilar cells 48 hours **(B)** following blast. No cells were apparent in the hilus one **(C)** and two **(D)** weeks following blast injury. IML=inner molecular layer, GCL=granule cell layer, H=hilus. Scale bars= 100 microns.

In addition to calretinin the calcium-binding protein, parvalbumin, was used to indirectly assess changes in calcium following bTBI. However, unlike calretinin, no changes occurred following the recovery time points examined (Figure 3-2). The slight difference in staining intensity across each time point can be attributed to normal variation in immunocytochemistry.

The morphology of the cells present throughout the hilus and granule cell layer, as well as the density of processes does not change between sham and animals exposed to blasts (Figure 3-2).

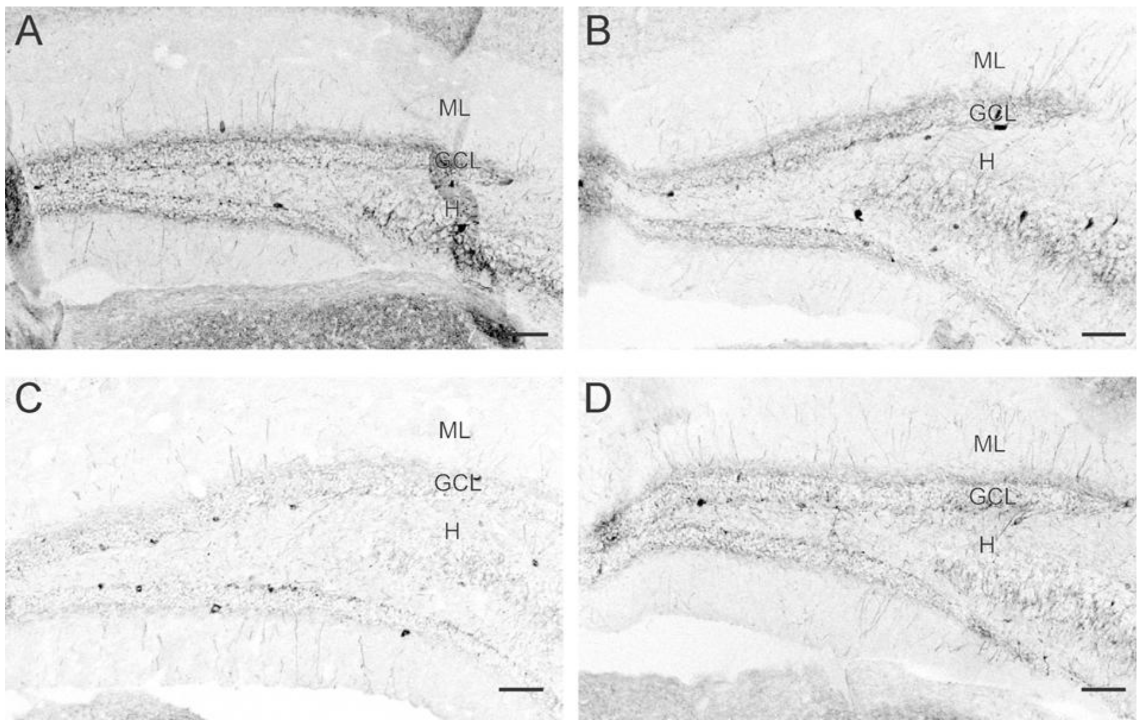

Figure 3-2. Time course of parvalbumin expression in the dentate gyrus following bTBI in animals anesthetized with ketamine, xylazine, and buprenorphine. No detectable difference in staining pattern was observed in the dentate gyrus of mice following blast injury compared to sham at all time points examined **(A).** Sham **(B).** 48 Hours **(C).** One Week and **(D).** Two Weeks following injury. ML=molecular layer, GCL=granule cell layer, H=hilus. Scale bars= 100 microns.

To determine the extent of glial activation the intermediate filament protein, GFAP found in the processes of astrocytes, was used. Widespread GFAP staining was observed throughout the dentate gyrus, with high density of hypertrophic processes in the granule cell layer, 48 hours following trauma (Figure 3-3B). Virtually no GFAP immunoreactivity was observed one and two weeks following blast (Figure 3-3C and D, respectively) compared to sham (Figure 3-3A). Of interest is the reduction in the intensity and density of astrocytes in the hilus and granule cell layer one and two weeks (Figure 3-3C and D) after injury compared to the basal GFAP levels seen in sham (Figure 3-3A).

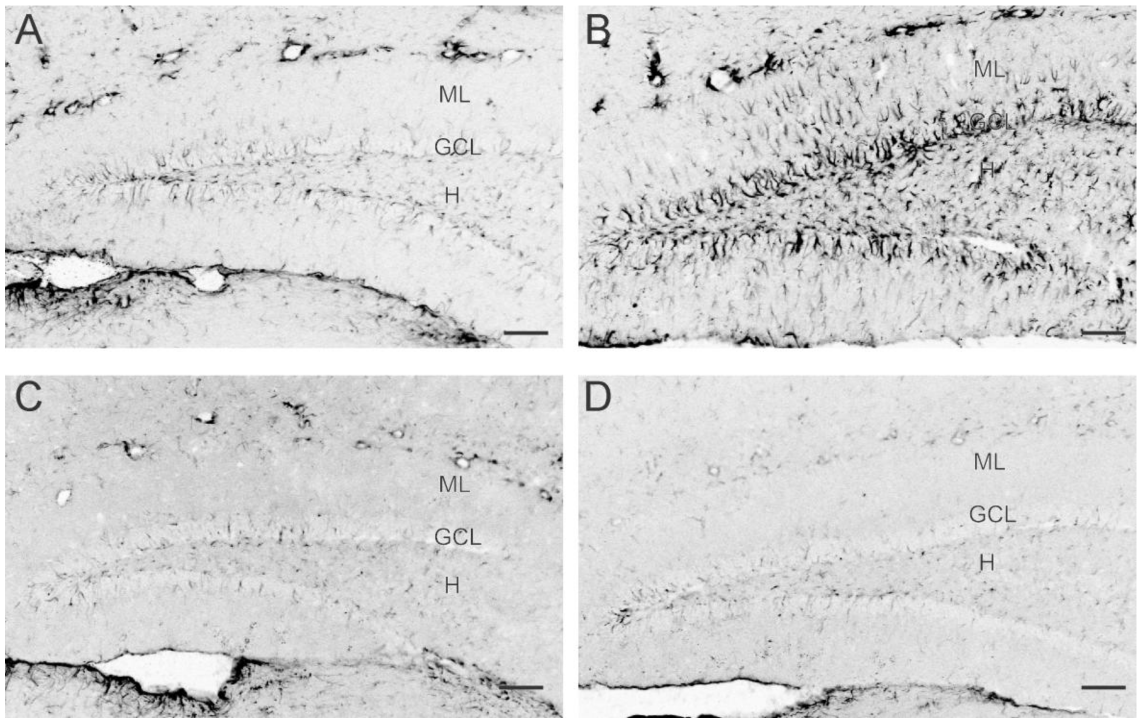

Figure 3-3. Time course of GFAP expression in the dentate gyrus following bTBI in animals anesthetized with ketamine, xylazine, and buprenorphine. Compared to sham **(A)** widespread activation of astrocytes throughout the dentate gyrus was most obvious 48 hours following blast injury **(B).** Reduction in GFAP was observed one week **(C)** and two weeks **(D)** following injury. **(A).** Sham **(B).** 48 Hours **(C).** One Week and **(D).** Two Weeks following injury. GFAP=glial fibrillary acidic protein. ML=molecular layer, GCL=granule cell layer, H=hilus. Scale bars= 100 microns.

A slight increase in the number of doublecortin positive somata was observed 48 hours following blast (Figure 3-4B) compared to sham (Figure 3-4A). Interestingly, although the number of somata appears to increase 48 hours following blast the density and length of dendritic processes in animals subjected to blast is reduced. The amount of labeled somata following a one and two week recovery (Figure 3-4C and D, respectively) did not change in comparison to doublecortin staining following 48 hours. However, there is less intense labeling of the somata. In addition, density and length of dendrites extending throughout the granule cell layer and molecular layer are further reduced compared to the staining seen following the 48 hour recovery (Figure 3-4C and D).

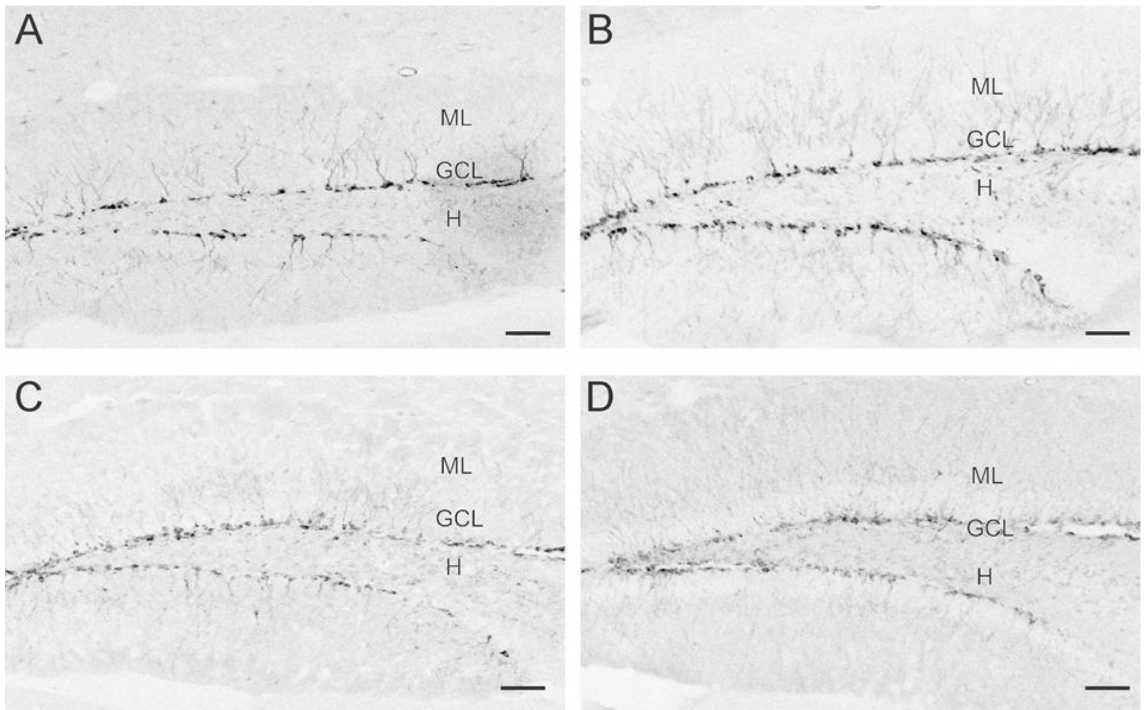

Figure 3-4. Time course of doublecortin expression in the dentate gyrus following bTBI in animals anesthetized with ketamine, xylazine, and buprenorphine. Compared to sham **(A)** an increase in labeled somata and processes containing for doublecortin was observed 48 hours following blast injury **(B)**. The same increase in somata was seen one **(C)** and two **(D)** weeks following trauma however there was a reduction in intensity as well as a decrease in dendritic arbors compared to sham **(A)** and the 48 hour recovery **(B).** ML=inner molecular layer, GCL=granule cell layer, H=hilus. Scale bars= 100 microns.

Influence of Anesthetics

The sham mice used were anesthetized with ketamine and xylazine followed by the analgesic buprenorphine. Because of this, a direct comparison can only be made between sham animals and mice blasted with the full drug cocktail. Additional shams are needed for animals blasted with buprenorphine and xylazine as well as xylazine only. However, data from animals receiving buprenorphine and xylazine as well as xylazine only have been included to compare differences in blast response with anesthetics.

There were differences observed in calretinin staining within the dentate gyrus across different drug combinations. A notable increase in calretinin staining of the inner molecular layer was observed in mice receiving ketamine, xylazine and buprenorphine (Figure 3-5B). A gradual reduction in the number of labeled hilar cells correlated with decreases in the types of anesthetics administered. Animals given all drugs had the most intense staining (Figure 3-5B) while those receiving xylazine and buprenorphine (Figure 3-5C) have less intense staining followed by the least intense staining in animals given xylazine only (Figure 3-5D). Interestingly, hilar cells were virtually undetected in mice receiving xylazine only (Figure 3-5D).

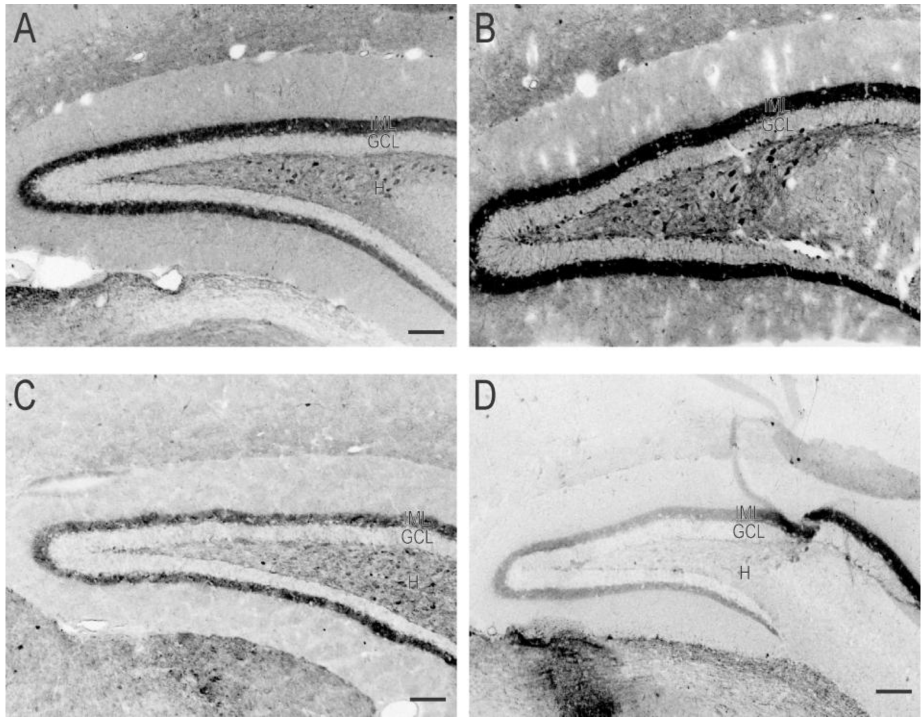

Figure 3-5. Calretinin expression in the dentate gyrus varies with anesthetics 48 hours following blast injury. Mice anesthetized with ketamine and xylazine, followed by buprenorphine administration show higher intensity of staining in the inner molecular layer as well as an increase in the number of hilar cells **(B)** in comparison to sham receiving all drugs **(A)**. Expression of calretinin in mice given xylazine and buprenorphine **(C)** decreases slightly below sham **(A)**. The reduction in staining intensity below sham is more pronounced in mice receiving xylazine only **(D)**. ML=molecular layer, GCL=granule cell layer, H=hilus. Scale bars=100microns.

Widespread GFAP staining, indicative of astrogliosis, was observed throughout all layers of the dentate gyrus, particularly in the granule cell layer, after injury in mice receiving ketamine, xylazine and buprenorphine (Figure 3-6B) compared to sham (Figure 3-6A). Little GFAP immunoreactivity was seen in mice anesthetized with xylazine and buprenorphine (Figure 3-6C) or just xylazine only (Figure 3-6D).

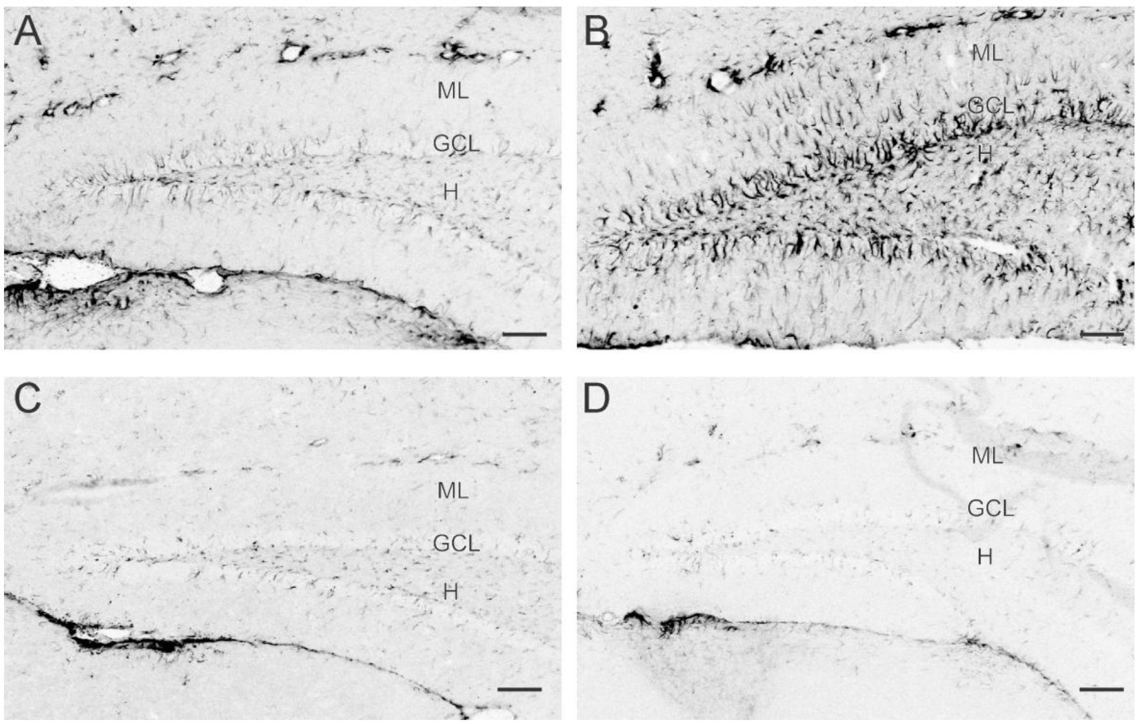

Figure 3-6. Differences in GFAP expression varies with anesthetics in the dentate gyrus following bTBI. Administration of ketamine and xylazine followed by buprenorphine **(B)** showed widespread astrogliosis throughout the dentate gyrus compared to sham **(A)**, and compared to mice anesthetized with buprenorphine and xylazine **(C)** or just xylazine only **(D)**. ML=molecular layer, GCL=granule cell layer, H=hilus, GFAP=glial fibrilary acidic protein. Scale bars= 100 microns.

Similar staining patterns such as density of processes and cell types was observed throughout the dentate gyrus of mice administered ketamine, xylazine and buprenorphine (Figure 3-7B) compared to buprenorphine and xylazine (Figure 3-7C). However, mice that received xylazine only showed increased parvalbumin in the granule cell layer and mossy fiber within the hilus (Figure 3-7D).

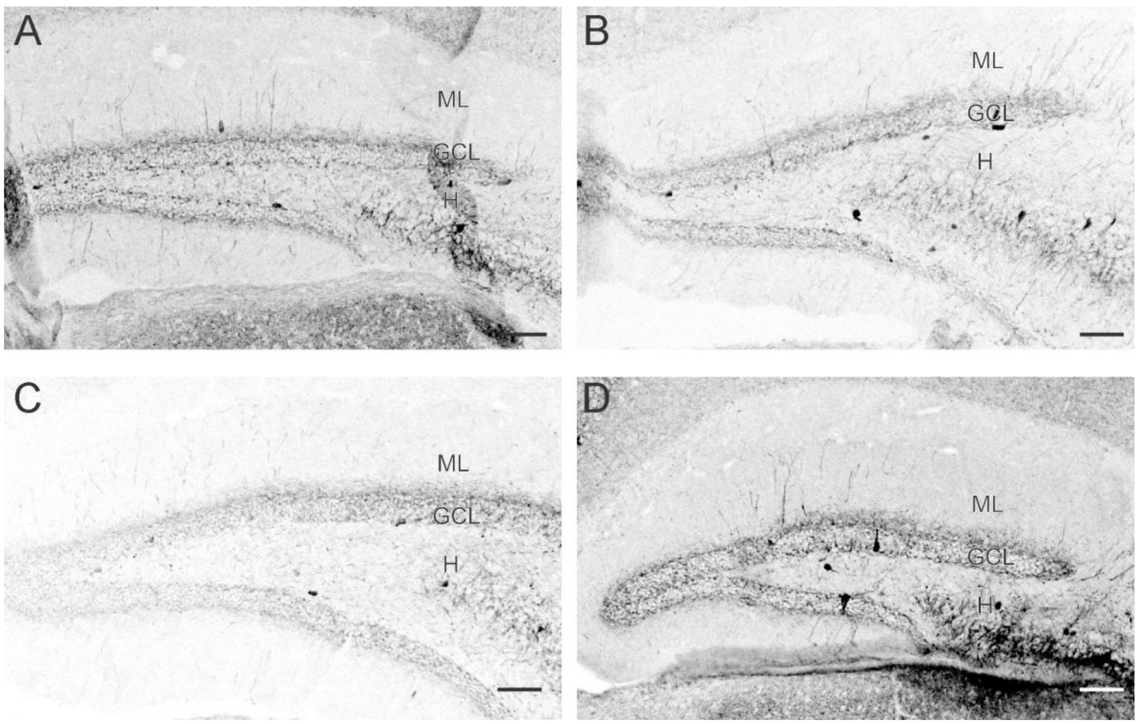

Figure 3-7. Use of different anesthetics shows slight differences in parvalbumin expression in the dentate gyrus following bTBI. There was a slight increase in parvalbumin immunoreactivity in the GCL and a large increase in the mossy fiber layer of mice treated with just xylazine only **(D)** compared to all other drug combinations. **(A).** Sham **(B).** Ketamine, xylazine, buprenorphine **(C).** Xylazine and buprenorphine **(D).** Xylazine only**.** ML=molecular layer, GCL=granule cell layer, H=hilus. Scale bars= 100 microns.

Doublecortin immunoreactivity differed with drug combinations (Figure 3-8). There was a faint increase in doublecortin in somata and processes in blasted mice receiving ketamine, xylazine and buprenorphine (Figure 3-8B) compared to sham (Figure 3-8A). Surprisingly, there was a large reduction in overall doublecortin immunoreactivity in animals administered xylazine and buprenorphine (Figure 3-8C). A reduction decrease in staining intensity and number of cells also occurred in mice treated with xylazine only (Figure 3-8D).

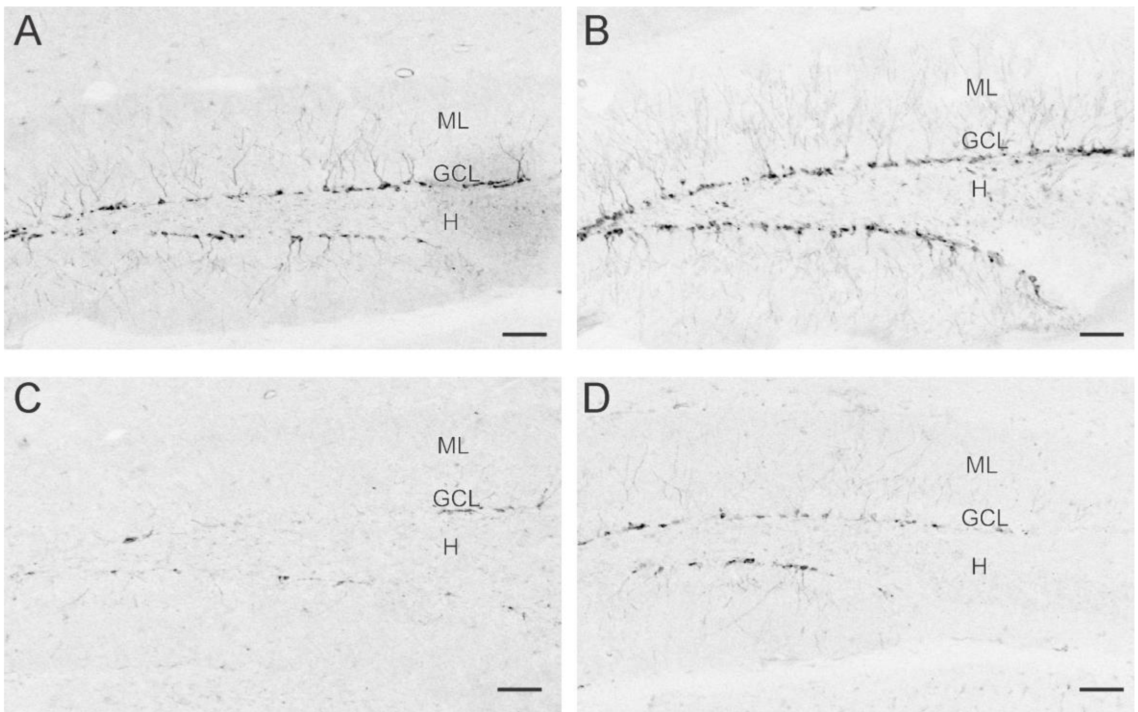

Figure 3-8. Effect of different anesthetics on doublecortin expression in the dentate gyrus following bTBI. An increase in somata and processes containing doublecortin was seen 48 hours following blast in animals receiving ketamine, buprenorphine and xylazine **(B)** compared to sham **(A)**. However, staining was considerably reduced in mice that received buprenorphine and xylazine **(C)** or xylazine only **(D)**. Scale bars= 100 microns.

Chapter 4

Response of bTBI in the RSC

Effect of Recovery Time Following Trauma

Immunocytochemical analysis of the two calcium-binding proteins, calretinin and parvalbumin, differed in response to blast injury in the RSC over the recovery times examined.

Cell counting analysis performed on parvalbumin data show an increase in the average number of parvalbumin positive interneurons. The greatest increase occurred 48 hours following injury (Figure 4-1A). Although the average number of parvalbumin containing cells increase one and two weeks following trauma the level of increase is not much greater than sham (Figure 4-1A). Immunostaining shows no change in morphology of cells positive for parvalbumin (Figure 4-1B-E). Interestingly, there was an increase in the intensity of staining in parvalbumin positive cells following 48 hours (Figure 4-1C) compared to any other time point.

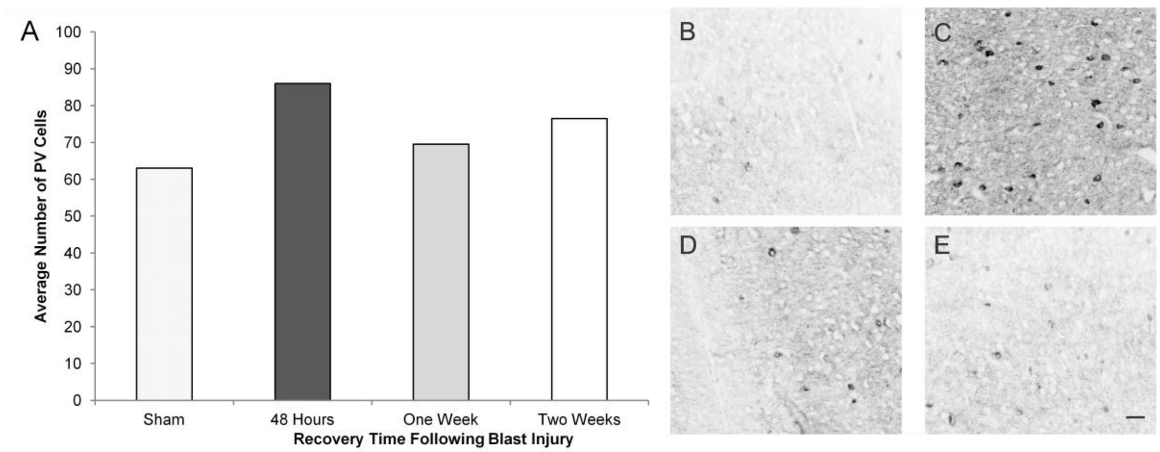

Figure 4-1. Increased expression and average number of parvalbumin cells in the RSC following bTBI in animals anesthetized with ketamine, xylazine and buprenorphine. The largest increase in parvalbumin occurred 48 hours following trauma **(A)**. No changes in cell types expressing parvalbumin was seen at 48 hours **(C)**, one week **(D)** or two weeks **(E)** compared to sham **(B)** but there was an increase in the intensity in parvalbumin positive cells. Sham (n=3), 48 Hours (n=2), One Week (n=2), Two Weeks (n=2). PV= parvalbumin. Scale bar= 100 microns for all images.

There was not a noticeable increase in calretinin staining following the 48 hour recovery (Figure 4-2A). Like parvalbumin, the average number of calretinin cells was similar one and two weeks following injury. However, the average number of cells one and two weeks after blast compared to sham show a large decrease.

Although no differences were seen in morphology of cells stained with calretinin (Figure 4-2B-E) there is a noticeable increase in staining intensity 48 hours (Figure 4-2C) following bTBI.

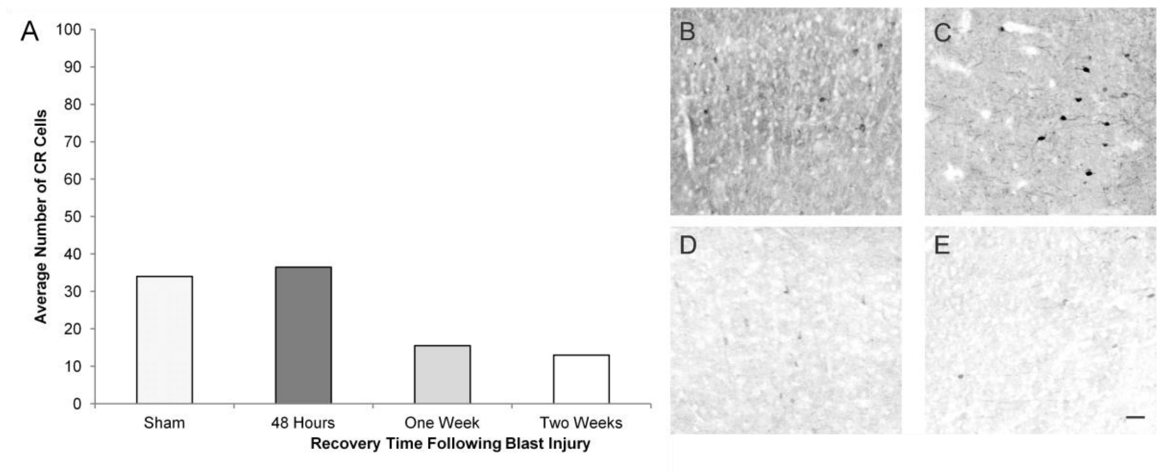

Figure 4-2. Changes in calretinin expression over time following bTBI in the RSC of mice anesthetized with ketamine, xylazine and buprenorphine. Compared to sham **(B)** there was a large reduction in the number of calretinin positive cells at one **(D)** and two weeks **(E)** following blast injury.The number of calretinin positive cells increased slightly 48 hours (dark gray) following trauma. **B-E** show no difference in the cell types expressing calretinin following injury. Sham (n=3), 48 Hours (n=2), One Week (n=2), Two Weeks (n=2). CR=calretinin. Scale bar= 100 microns.

Overall, the intermediate filament, GFAP, show virtually no astrogliosis following any of the recovery times studied (Figure 4-3). However, there was some astrocytic activation present in the central region of the RSC 48 hours following blast (Figure 4-3B, square inset).

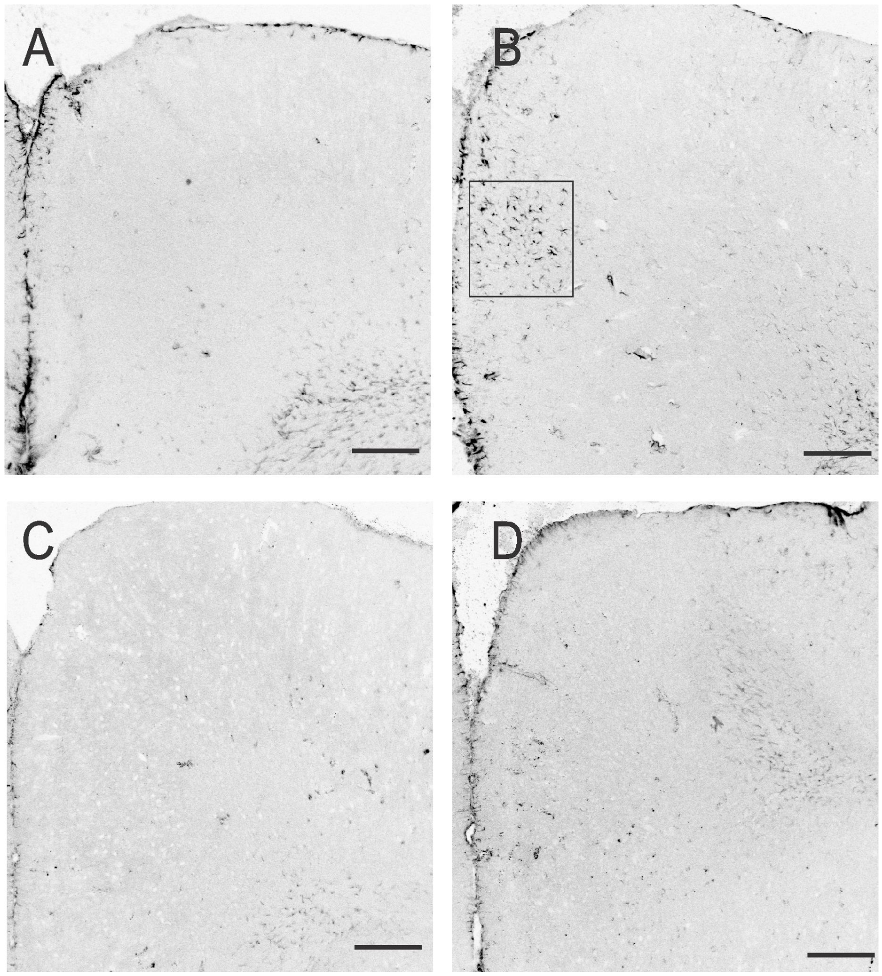

Figure 4-3. No widespread astrogliosis observed following acute and chronic recovery from bTBI in the RSC in animals anesthetized with ketamine, xylazine and buprenorphine. The central region of the RSC shows some activated asctrocytes after 48 hours **(B. square inset)** whereas GFAP is virtually undetectable in sham **(A)** and at one and two weeks **(C, D respectively)** following trauma. GFAP=glial fibrillary acidic protein. Scale bar=200 microns.

Influence of Anesthetics

The sham mice used were anesthetized with ketamine and xylazine followed by the analgesic buprenorphine. Because of this, a direct comparison can only be made between sham animals and mice blasted with the full drug cocktail. Additional shams are needed for animals blasted with buprenorphine and xylazine as well as xylazine only. However, data from animals receiving buprenorphine and xylazine as well as xylazine only have been included to compare differences in blast response with anesthetics.

An increase in the average number of parvalbumin cells occurred in mice administered ketamine, xylazine and buprenorphine compared to sham animals that also received the full drug cocktail (Figure 4-4A). Overall, there was not a large difference in the average number of parvalbumin positive cells among animals receiving different drug combinations.

No differences in cell morphology were observed in animals administered different drugs (Figure 4-4B-E), however, the intensity of staining was greatest in blasted animals receiving all drugs (Figure 4-4C) compared to mice that were given xylazine and buprenorphine (Figure 4-4D) or xylazine only (Figure 4-4E).

Unlike parvalbumin, differences in drug combinations had no effect on the average number of calretinin positive cells in the RSC 48 hours after blast (Figure 4-5B). Furthermore, there was no difference in morphology or staining intensity of calretinin positive cells across groups (Figure 4-5B-E).

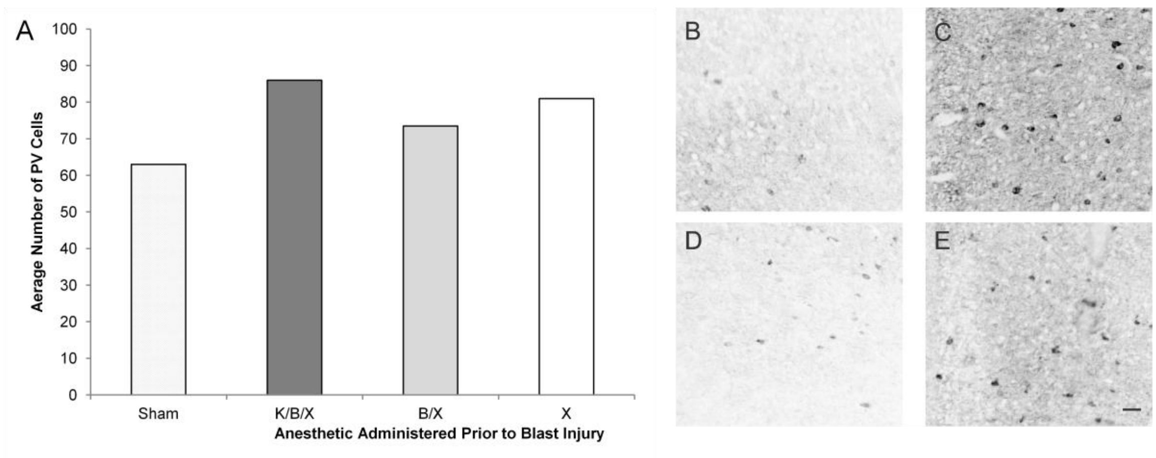

Figure 4-4. Increase in the number of parvalbumin cells 48 hours after bTBI regardless of anesthetic in the RSC. (A) Although all anesthetics tended to increase parvalbumin, the greatest increase was seen in mice administered ketamine and xylazine followed by buprenorphine (dark gray). No morphological changes were seen in the cells expressing parvalbumin **(C-E)** between any anesthetic compared to sham **(B)**. K=ketamine, B=buprenorphine, X=xylazine. **B.** Sham (n=3), **C.** K/B/X (n=2), **D.** B/X (n=2), **E.** X (n=2). PV=parvalbumin. Scale bar=100 microns for all images.

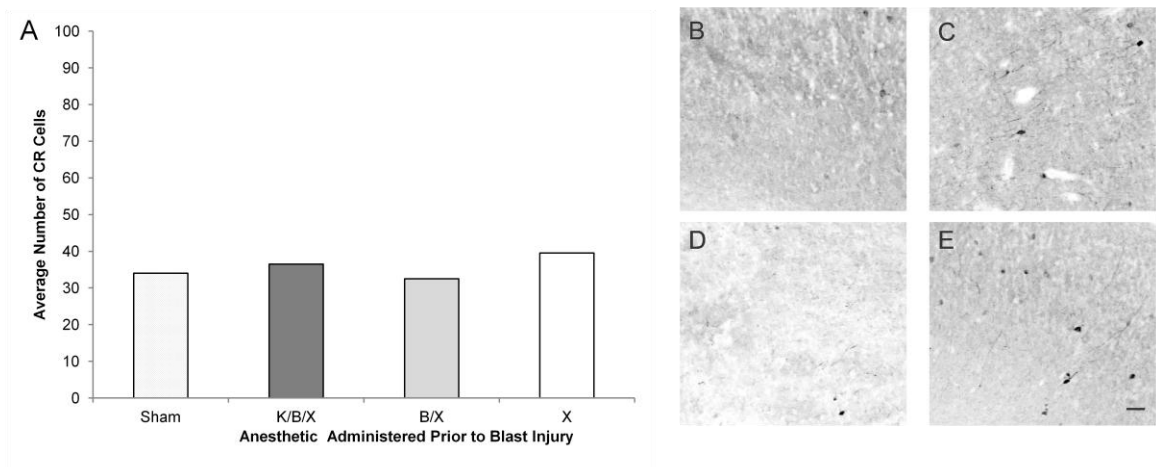

Figure 4-5. Changes in calretinin expression with different anesthetics in the retrosplenial cortex. (A) slight increase occurred in the number of calretinin calls in mice treated with xylazine only (white bar) compared to sham. No changes were seen in cell morphology of calretinin positive cells **(B-E)**. K=ketamine, B=buprenorphine, X=xylazine. **B.** Sham (n=3), **C.** K/B/X (n=2), **D.** B/X (n=2), **E.** X (n=2). CR=calretinin. Scale bar=100 microns for all images.

There was little astrocytic activation among the different anesthetics (Figure 4-6). Animals that received all drugs showed slight astrocytic activation in the central region of the RSC (Figure 4-6, square inset). GFAP staining was virtually undetected in animals that received xylazine and buprenorphine as well as animals receiving xylazine only (Figure 4-6C and D, respectively).

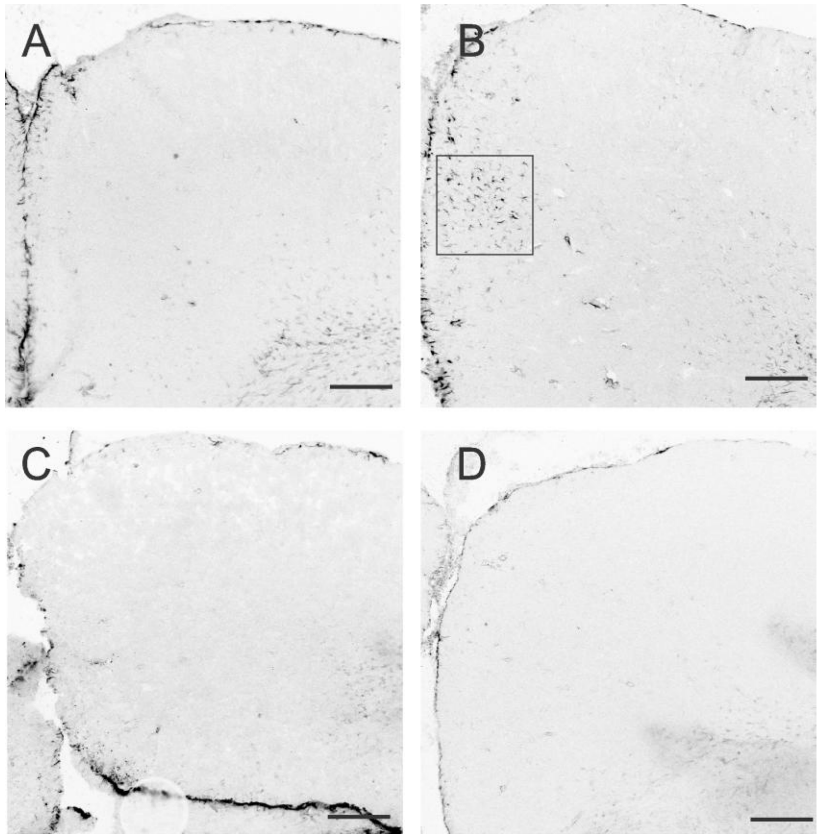

Figure 4-6. No widespread astrogliosis observed following bTBI regardless of anesthetic administered in the RSC. GFAP is virtually undetectable in sham **(A)**, and in mice treated with B/X or just X **(C, D respectively)**. However in mice administered all drugs the central region of the RSC shows activated asctrocytes **(B. square inset)**. K=ketamine, B=buprenorphine, X=xylazine. GFAP=glial fibrillary acidic protein. Scale bars=200 microns.

Chapter 5

Response to bTBI in the visual cortex

Effect of Recovery Time Following Trauma

The average number of parvalbumin positive cells in animals that recovered 48 hours from blast, on average, showed a two-fold increase compared to sham (Figure 5-1A). In animals that recovered one and two weeks following blast injury there was virtually no difference in the average number of parvalbumin positive cells in the visual cortex.

There were no changes in cell morphology across any of the recovery times examined (Figure 5-1B-E). However, there appeared to be a decrease in staining intensity one and two weeks following injury (Figure 5-1C and D, respectively) compared to sham and the 48 hour recovery (Figure 5-1B and C, respectively).

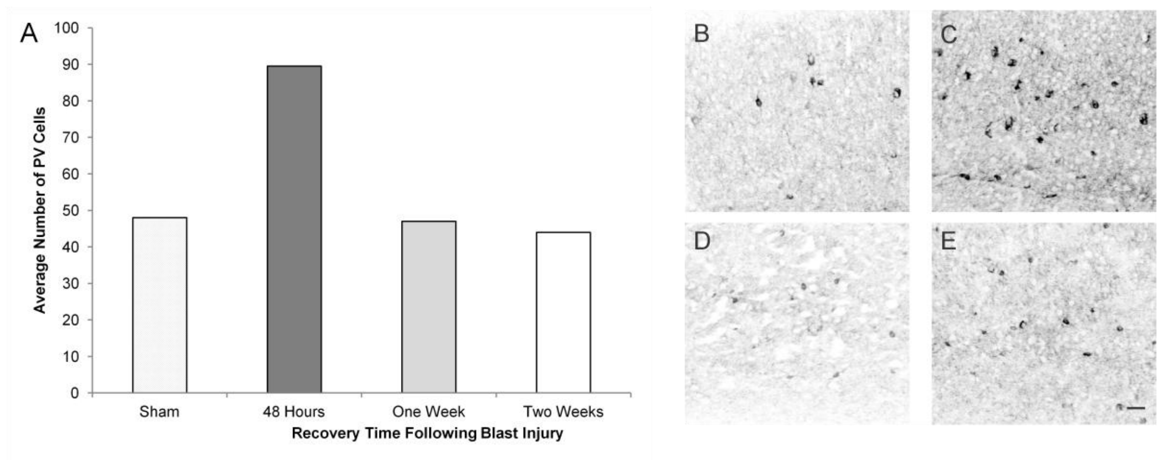

Figure 5-1. Changed in the average number of parvalbumin positive cells in the visual cortex at different time points following blast injury. A substantial increase in parvalbumin was seen 48 hours after blast injury compared to sham **(A)**. No changes in morphology of cells were seen **(B-E)**. **B.** Sham (n=3) **C.** 48 Hours (n=2) **D.** One Week (n=2) **E.** Two Weeks (n=2). PV=parvalbumin. Scale bars=100 microns for all images.

For calretinin, the only noticeable change was the reduction in cells two weeks after injury compared to sham (Figure 5-2). A slight increase in the average number of calretinin positive cells occurred 48 hours following blast compared to sham (Figure 5-2). However, there was no difference in the average number of calretinin positive cells one week after injury compared to sham.

There were no differences in morphology or intensity in cell containing calretinin (Figure 5-3A and B). However, varicosities throughout the processes of calretinin positive cells were widespread in the visual cortex 48 hours following injury (Figure 5-3, B1 arrows) compared to sham processes that appeared smooth and continuous (Figure 5-3A1).

Levels of GFAP were undetected in the visual cortex over the recovery times observed (Figure 5-4).

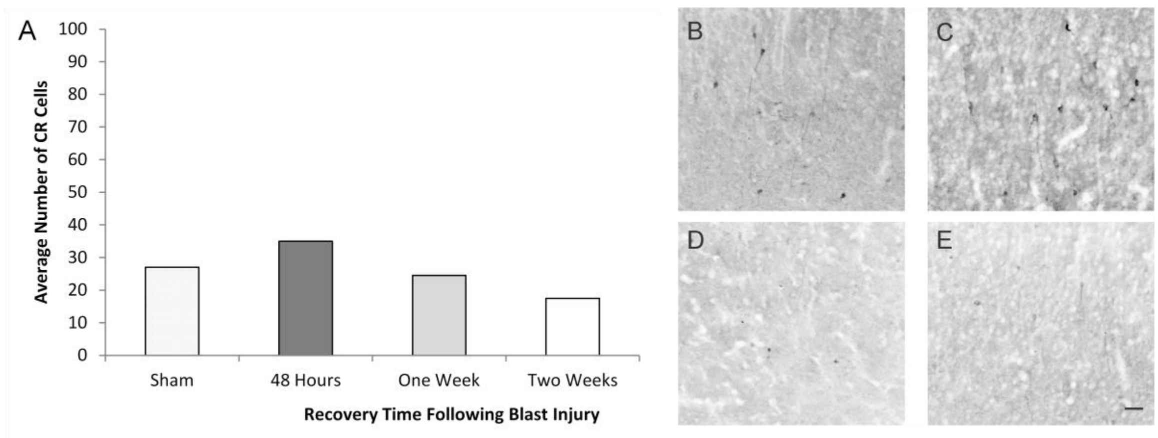

Figure 5-2. Number of Calretinin positive cells decreases with time following blast in animals anesthetized with ketamine, xylazine and buprenorphine. The largest decrease was seen at two weeks **(A)**. Representative images **(B-E)** show no change in cell type. **B.** Sham (n=3), **C.** 48 Hours (n=2), **D.** One Week (n=2), **E.** Two Weeks (n=2) CR=calretinin. Scale bar=100 microns for all images.

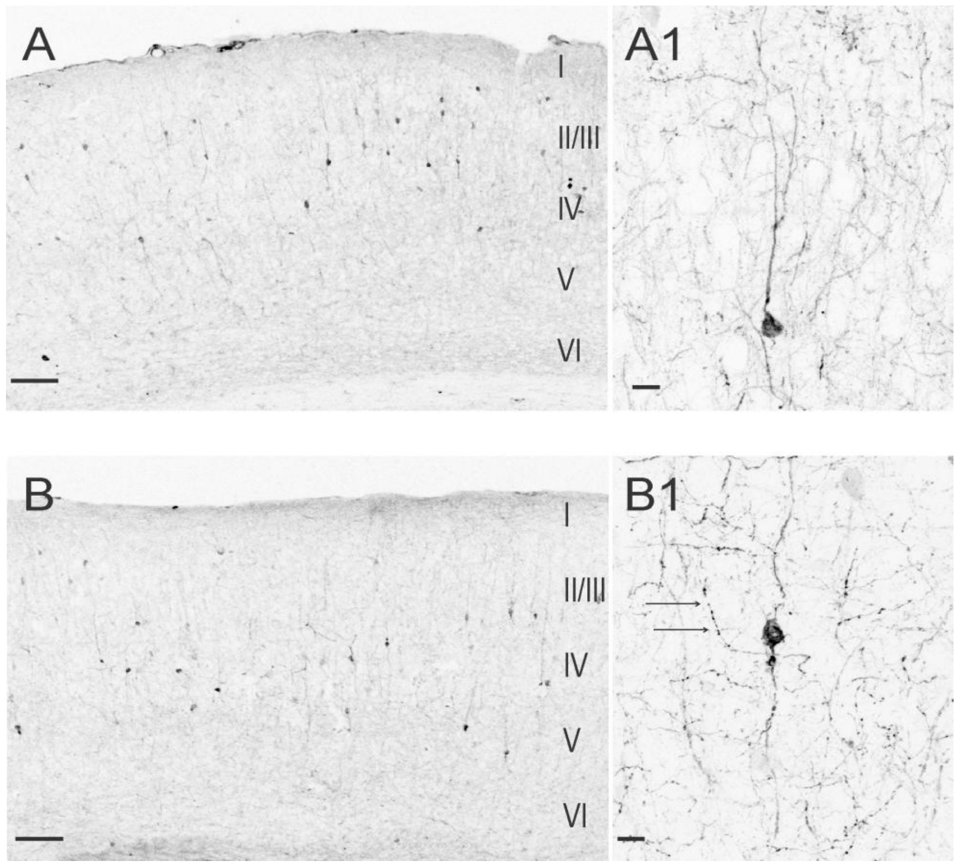

Figure 5-3. Varicosities in the processes of calretinin positive neurons 48 hours following bTBI. No change in cell types was observed between sham **(A, A1)** and 48 hour blast **(B, B1)**. However, varicosities were observed in the processes of bipolar cells in the visual cortex of mice following 48 hour recovery **(B1, arrows)**. Scale bars=200 microns **(A and B)**, Scale bars=100 microns **(A1 and B1)**.

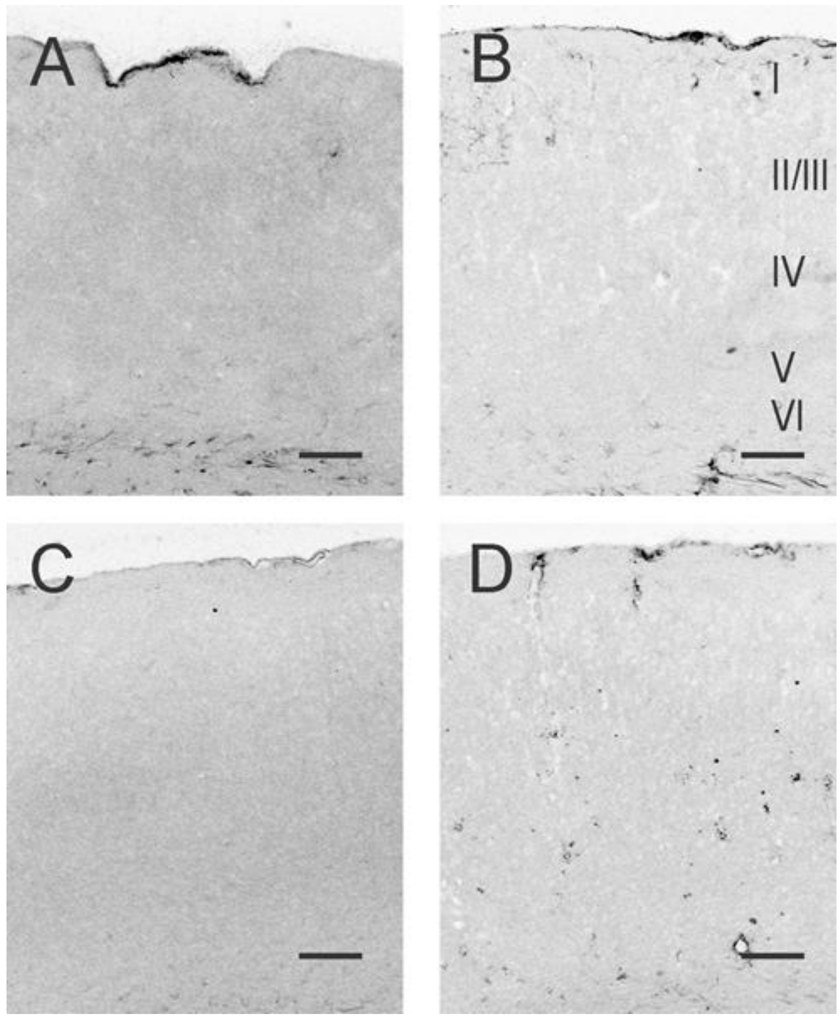

Figure 5-4. GFAP staining reveals no activation of astrocytes in the visual cortex at any time points examined following injury. (A). Sham **(B).** 48 Hours **(C).** One Week and **(D).** Two Weeks following injury. GFAP=glial fibrillary acidic protein. Scale bars=200 microns.

Influence of Anesthetics

The sham mice used were anesthetized with ketamine and xylazine followed by the analgesic buprenorphine. Because of this, a direct comparison can only be made between sham animals and mice blasted with the full drug cocktail. Additional shams are needed for animals blasted with buprenorphine and xylazine as well as xylazine only. However, data from animals receiving buprenorphine and xylazine as well as xylazine only have been included to compare differences in blast response with anesthetics.

The average number of cells containing parvalbumin increases two-fold in animals receiving ketamine, buprenorphine and xylazine compared to sham (Figure 5-5).There was no difference in the average number of parvalbumin cells between mice treated with a combination of xylazine and buprenorphine versus xylazine only but compared to animals blasted with the full drug cocktail the difference was prominent (Figure 5-5A).

No changes in cell type or staining intensity occurred in parvalbumin with the different drug combinations (Figure 5-5B-E).

The number of calretinin positive cells increased gradually as the number of drugs administered decreased (Figure 5-6). Similar to parvalbumin there was no change in morphology or staining intensity of calretinin positive cells (Figure 5-6B-E).

GFAP staining was nearly undetectable in across all drug combinations (Figure 5-7A-D). However, faint immunoreactivity for activated astrocytes was localized throughout a small area of layers 2 and 3 in mice administered xylazine only (Figure 5-7D).

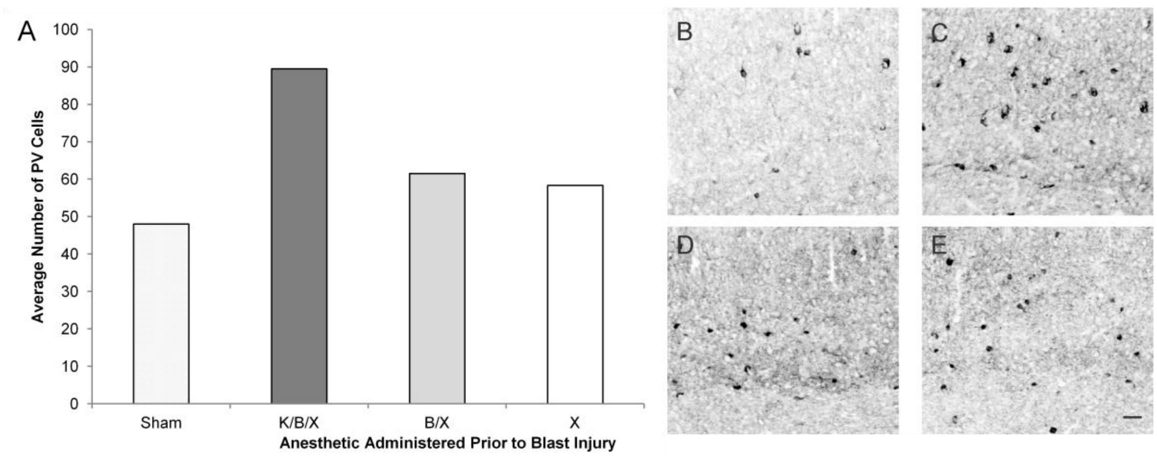

Figure 5-5. Differences in the average number of parvalbumin cells with different anesthetics in the visual cortex. There was an increase in cells with parvalbumin mice treated with K/B/X compared to sham **(A)**. Representative cells shown in **B-E**. No change in morphology of parvalbumin cells was observed with differences in anesthetic. K=ketamine, B=buprenorphine, X=xylazine. **B.** Sham (n=3), **C.** K/B/X (n=2), **D.** B/X (n=2) **E.** X (n=2). PV=parvalbumin. Scale bar= 100 microns for all images.

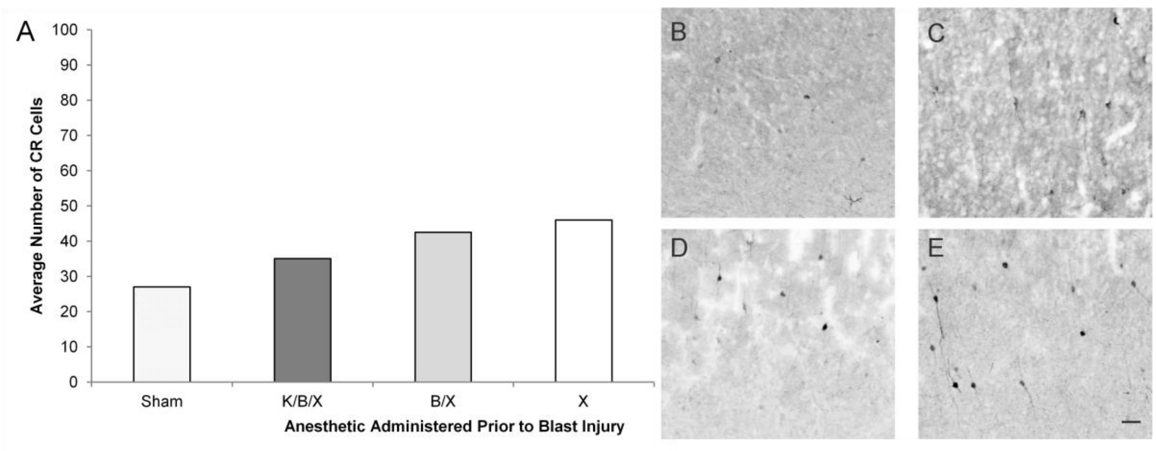

Figure 5-6. There was a tendency for increased numbers of calretinin positive cells with fewer anesthetics. No difference was seen in cell types containing calretinin **(B-E)**. K=ketamine, B=buprenorphine, X=xylazine. **B.** Sham (n=3), **C.** K/B/X (n=2), **D.** B/X (n=2), **E.** X (n=2). CR=calretinin. Scale bar=100 microns for all images.

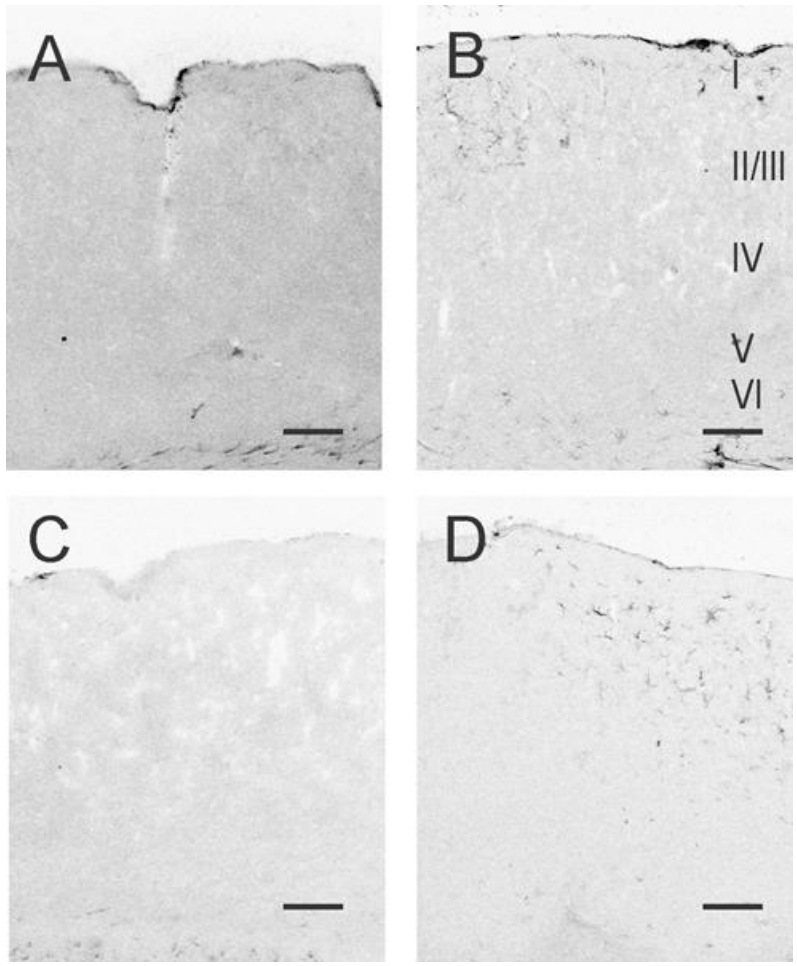

Figure 5-7. GFAP staining reveals no activation of astrocytes in the visual cortex with different anesthetics following blast injury. (A). Sham **(B).** Ketamine, buprenorphine, xylazine **(C).** Buprenorphine, xylazine **(D).** xylazine only. GFAP=glial fibrillary acidic protein. Scale bars=200 microns.

Chapter 6

DISCUSSION

A major challenge in TBI progress has been the complication of injuries sustained from transmission of blast waves through gas filled cavities (e.g. lungs) and vessels (Kuehn et al., 2011). Historically, primary damage resulting from blast waves have been unacknowledged due to theories of the skull providing sufficient protection against damaging blast waves (Clemedson, 1956). Only recently has use of blast injury models become increasingly accepted in its applicability to damages sustained (Cernak & Noble-Haeusslein, 2010). The results of my work provide additional evidence that bTBI is a valid model to study the subtle effects of TBI. Because blasts were directed exclusively to the head of all animals injury observed can be confidently presumed to result solely from blast pressures.

Differential response of the calcium-binding proteins calretinin and parvalbumin

A number of TBI related pathologies (Parkinson’s Disease, Alzheimer’s Disease, epilepsy and schizophrenia) involve excitotoxicity, resulting in increased intracellular calcium, as one of the major insults (Buritica *et al.*, 2009). Interneurons are widely studied targets of these pathologies. Representing 20-30% of the neuronal population in the mammalian cortex, interneurons have an important role in regulating neuronal circuits (Barinka & Druga, 2010). Most are inhibitory and use gamma-aminobutyric acid (GABA) as their neurotransmitter. Non-overlapping populations of interneurons have been identified using staining for different calcium-binding proteins (Baimbridge et al., 1992, Barinka & Druga, 2010). Because these studies did not directly address inhibition involving GABA, there is only indirect insight into the relationship between calcium homeostasis and these inhibitory neurons.

Of the three brain regions I analyzed, the dentate gyrus showed the most prominent responses for all immunocytochemical markers used. The differential responses of calretinin and parvalbumin in the dentate gyrus were notable. Strong increases in calretinin occurred in the inner molecular layer and in hilar cells 48 hours following bTBI, while parvalbumin immunoreactivity following bTBI did not differ from sham animals. Based on the proximity to the blast, I hypothesized that staining of these calcium-binding proteins in the cortex would show the greatest response to blast injury. However changes in calcium-binding proteins in the cortex, especially the visual cortex were more subtle. The presence varicosities in the processes of calretinin positive cells are indicative of damage, as this type of blebbing has been reported to be a precursor of axonal disconnection and ultimately cell death (Ropper, 2011, Rosenfeld et al., 2013). The pronounced changes in the dentate gyrus compared to the retrosplenial and visual cortices may be attributed to acceleration/deceleration or rotational forces that culminate into inertial forces that damage brain regions not in the immediate vicinity of blast waves (Greve & Zink, 2009).

As previously mentioned, one of the main secondary insults resulting from TBI is excitotoxicity from imbalances in calcium homeostasis (Greve & Zink, 2009). Based on this knowledge, I hypothesized that an increase in both calcium-binding proteins would occur. Initially the magnitude of increase in calretinin and the lack of change in parvalbumin were surprising until the kinetic properties of each were considered.

Parvalbumin acts as a slow buffer whereas calretinin has been reported to function as a fast buffer, although it does have some similarities with other calcium buffers (e.g. calbindin) also allowing it to act as a slow buffer (Barinka & Druga, 2010, Schwaller, 2010). My results suggest that acutely following blast injury any substantial rise in intracellular calcium may be adequately buffered by calretinin such that levels of parvalbumin do not need to increase. The rise in calretinin following injury has been reported previously (Camp & Wijesinghe, 2009). Much of this has been centered on the possibility of calretinin having a neuroprotective role (D'Orlando *et al.*, 2002). Although many of the reports citing the possibility of calretinin exerting neuroprotection have centered on tissue and cell cultures, the findings have been convincing. For example, D’Orlando et al. (2000) showed evidence of cells possessing calretinin being spared from degeneration resulting from delayed calcium dependent L-glutamate-induced cytotoxicity.

The dramatic difference in calretinin levels at 48 hours versus one and two weeks following blast warrants examining additional recovery time points. Although it is unusual for calcium to decrease following injury, it is possible the subsequent decrease in calretinin may be due to the activation of unknown compensatory mechanisms that caused a stabilization or reduction in calcium levels that ultimately reduced calretinin expression below sham levels. In addition to examining a more extensive time course between 48 hours and one week, it would be of interest to determine how immediate the increase in calretinin is following blast and whether levels of parvalbumin remain unchanged. Studies have shown alterations in calcium as early as three hours following injury (Weber *et al.*, 2001).

Release of the excitatory amino acid glutamate and the production of free radicals and nitric oxide are detrimental processes closely linked with imbalances in calcium homeostasis (Greve & Zink, 2009). It would be of interest to measure the levels of these molecules and in relation to the severity of excitoxicity. Furthermore, although elevation in intracellular calcium levels can lead to a number of secondary cascades ultimately resulting in cell death (Weber, 2012), the implication of calretinin having a neuroprotective effect is worth exploring. Examining markers such lactate dehydrogenase (LDH), an enzyme useful in quantifying necrosis, calpains and proteases known to be involved in pathological end points would help determine the ultimate fate of cells following blast injury.

Increased neurogenesis following bTBI

Increases in neurogenesis are believed to underlie repair to damaged hippocampal circuits following injury (Kernie & Parent, 2010, Sun *et al.*, 2007, Dash et al., 2001). Sun et al. (2007) have shown that newly synthesized and integrated granule cells are associated with improvements in cognition following TBI (Sun et al., 2007). Thus the increase in doublecortin I saw 48 hours following bTBI is consistent with several studies that report increases in neurogenesis following brain injury (Yu et al., 2008, Kernie & Parent, 2010, Dash et al., 2001). Lack of a persistent increase in doublecortin staining at one and two weeks following injury was unexpected, as enhanced neurogenesis has been shown to persist as long as six months following trauma (Kernie & Parent, 2010). Because staining at these later time points was not drastically reduced compared to sham, it is possible that since this was only mild TBI, only a brief increase in neurogenesis was required. The analysis of a larger sample size and a more detailed analysis of different time points might clarify the situation.

Although several models of TBI show increased neurogenesis, the mechanisms producing these increases have not been elucidated (Kernie & Parent, 2010). There are a number of molecules released during injury that may play a role in initiating neurogenesis making the induction of neurogenesis, especially as it relates to TBI a challenge to study. Two molecules that have gained recognition are glutamate and KCl (Kernie & Parent, 2010, Shi *et al.*, 2007, Mattson, 2008). Glutamate's role in regulation of neurogenesis has been linked to its effect on calcium influxes that can result in transcriptional changes leading to neurogenesis (Mattson, 2008). Shi et al. (2007) proposed that neurogenesis is likely to involve voltage gated potassium channels (specifically Kv4.1) based on increased stem cell proliferation following administration of exogenous KCl to Bax-deficient mice. In addition, the activation of astrocytes and microglia have also been reported to secrete substances (growth factors and substances known to have immunological function) that influence neurogenesis (Myer *et al.*, 2006). Adding to the complexity in understanding neurogenic mechanisms is the fact that many of the molecules implied to have a role in stimulating neurogenesis are also linked with TBI morbidities (e.g. glutamate in excitoxicity and inflammation resulting from astrogliosis).

At present it is not certain whether neurogenesis alone is sufficient to improve cognition (Kernie & Parent, 2010). Although many injury models report increased neurogenesis and cognitive improvements (Yu et al., 2008, Kernie & Parent, 2010), additional studies are needed to confirm this. Many of the current tools used to assess the extent of neurogenesis include markers that are also found in reactive astrocytes making it difficult to distinguish these astrocytes from stem cells in the dentate gyrus (Kernie & Parent, 2010, Myer et al., 2006). Because of this, future work exploring neurogenesis will likely rely on genetic manipulations. In addition it would be of great interest to explore whether the newly integrated neurons are fully functional, as aberrations such as epilepsy could explain why symptoms following TBI persist (Toader *et al.*, 2013). Transgenic work involving ablation of neurogenesis followed by close observation during recovery would offer fundamental insight (Kernie & Parent, 2010). Efforts employing the use of electron microscopy and electrophysiology would help in assessing the structural integrity and functionality of newly integrated neurons (Kernie & Parent, 2010, Sun et al., 2007).

Astrogliosis in the dentate gyrus with bTBI

The only brain region to experience widespread astrogliosis was the dentate gyrus. As with all the other cell markers employed, the 48 hour recovery showed the most prominent GFAP response to injury. The increased GFAP staining in the dentate gyrus following injury was expected as a number of studies have reported reactive astrogliosis in the dentate gyrus following TBI (Sosa *et al.*, 2013, Myer et al., 2006). The presence of reactive astrocytes plays an important role in glial scarring following severe brain injury that results in inflammation, chronic pain and neurotoxicity (Sofroniew, 2009).

It must be stressed that reactivity of astrocytes is highly dependent on the type and severity of the damage sustained (Sofroniew, 2009). This contextual basis of astrogliosis is due to the specific signaling cascades involved. There has not been adequate consensus on the significance of different times courses for changes in GFAP levels in different models of TBI. One study employing a cryogenic model reported increased GFAP 24 hours following trauma with a peak response three to four days following injury (Amaducci et al., 1981). Another study reported persistent astrogliosis up to ten months following injury (Sosa et al., 2013).

Lack of widespread astrogliosis throughout the RSC and visual cortex was unexpected. Although diminished reactivity could be attributed to blast being insufficient to elicit a response, Zhao et al. (2003) report a loss of astrocytes following TBI. In their FPI model, rats showed significant loss of GFAP (both in the intensity and complexity of processes) following acute recovery as early as 30 minutes, with a continual decline at 24 hours in addition to increases in neuron degeneration as demonstrated by Fluoro-Jade staining (Zhao *et al.*, 2003). They believed the reduction in astrocytes was due to the severe damage that was initiated soon after injury in regions most sensitive to insult (Liu *et al.*, 1999). Likewise Liu et al. (1999) also found a decline in astrocytes coupled with neuron degeneration in an ischemic model of brain injury.

Because I examined only highly localized regions, it would be important to sample areas more rostral and caudal to the RSC, visual cortex and dentate gyrus to assess regional changes in GFAP expression. It would also be worthwhile to follow up with examination of glutamine synthetase, a marker that identifies non-activated glia, to determine if there are changes in the number of astrocytes. Although it is not clear why GFAP was largely undetectable throughout most cortical regions examined, an examination of a larger sample size may provide valuable information.

Influence of anesthetics on bTBI

The time courses examined here provide evidence that most prominent changes in all three markers occurred following a 48 hour recovery period. Based on this, I used this time point to assess changes in immunostaining with different combinations of the widely used anesthetics ketamine and xylazine and the analgesic buprenorphine.

My preliminary results indicate that anesthetics could have an effect on the response to blast injury because there were differences in staining pattern and intensity in blasted animals receiving different anesthetics. However in order to definitively assess the influence of anesthesia I need shams administered the same combination of anesthetics.

Of the three regions examined, the greatest impact occurred within the dentate gyrus with ketamine appearing to have a large influence. Vulnerability of the dentate gyrus following TBI has been reported previously and a consensus for enhanced neurogenesis has been established (Geddes *et al.*, 2003, McCarthy, 2003, Lowenstein et al., 1992). However the decreases in neurogenesis in mice receiving just xylazine and buprenorphine or just xylazine suggest that ketamine may be actually increasing neurogenesis.

It is worth noting that on average, across all drug combinations, the levels of calcium-binding proteins either increased or did not differ greatly from sham animals. This could indicate all of these drugs may be neuroprotective by protecting against calcium excitotoxicity although a greater sample size is warranted. As mentioned in the results chapters sham animals receiving the same drug combinations will be essential.

Depending on the trauma model, the choice of whether to administer anesthetics and analgesic is not always optional in that CCI and FPI require anesthetics for the necessary surgery; but the type of anesthetic and analgesic combinations can be examined. Certain anesthetics may exert a higher level of neuroprotection than others and different combinations can increase or decrease protective effects. Large scale studies carefully exploring dosing to determine the thresholds of neuroprotection versus neurotoxicity across injury paradigms are lacking. Until such studies are performed the degree of drug interference on functional, molecular and behavioral outcomes will remain largely unknown. Because different TBI models are used to reproduce specific forms of injuries seen clinically, the need to standardize anesthetic and analgesic choices within TBI models is essential.

Future studies

As mentioned previously, the findings presented here are largely based on preliminary data in terms of limited sample sizes and larger sample sizes are required to draw more definitive conclusions. In addition, although the effects of anesthetics are shown to be a confounding factor, future studies with buprenorphine only, as well as no drugs will be necessary for a more complete analysis.

The 48 hour time point showed large changes for all the markers used. However the most sensitive brain region under the conditions used in this study was the dentate gyrus. I think it is unlikely that the level of cognitive deficits resulting from TBI is due solely to hippocampal injury. Given the large role that the RSC has in executive functioning and its projections to and from the hippocampus, I believe that more widespread changes may occur in this cortical region. Likewise, given the common complaints regarding a variety of visual impairments including light sensitivity and double vision, it is likely that other central visual pathways such as the superior colliculus, as well as visual cortex are involved in bTBI (Cheng & Povlishock, 1988, Cockerham et al., 2009). The effect of primary blast on the retina remains to be established and no studies have examined if damage to the retina can be extrapolated to higher brain regions. It is possible that the retinal effects of bTBI can be used to determine the severity of central effects.

Another paradigm to be examined would be exposure to repeated blasts. Realistically, soldiers, civilians and athletes are often subjected to repeated insults prior to receiving medical attention. Consideration of the recovery time between repeated insults should also be carefully considered. And lastly, because changes in behavior can manifest long after injury, long term follow up studies that also examine behavior in animal models of blast injury would be useful.

References

Adams, J. H., D. Doyle, I. Ford, T. A. Gennarelli, D. I. Graham and D. R. McLellan, 1989: Diffuse axonal injury in head injury: definition, diagnosis and grading. *Histopathology,* **15,** 49-59.

Alsop, D. C., H. Murai, J. A. Detre, T. K. McIntosh and D. H. Smith, 1996: Detection of acute pathologic changes following experimental traumatic brain injury using diffusion-weighted magnetic resonance imaging. *Journal of neurotrauma,* **13,** 515-521.

Amaducci, L., K. I. Forno and L. F. Eng, 1981: Glial fibrillary acidic protein in cryogenic lesions of the rat brain. *Neuroscience letters,* **21,** 27-32.

Amaral, D. G., H. E. Scharfman and P. Lavenex, 2007: The dentate gyrus: fundamental neuroanatomical organization (dentate gyrus for dummies). *Progress in brain research,* **163,** 3-22.

Andressen, C., I. Blumcke and M. R. Celio, 1993: Calcium-binding proteins: selective markers of nerve cells. *Cell and tissue research,* **271,** 181-208.

Baimbridge, K. G., M. R. Celio and J. H. Rogers, 1992: Calcium-binding proteins in the nervous system. *Trends in neurosciences,* **15,** 303-308.

Barinka, F. and R. Druga, 2010: Calretinin expression in the mammalian neocortex: a review. *Physiological research / Academia Scientiarum Bohemoslovaca,* **59,** 665-677.

Benson, R. R., S. A. Meda, S. Vasudevan, Z. Kou, K. A. Govindarajan, R. A. Hanks, S. R. Millis, M. Makki, Z. Latif, W. Coplin, J. Meythaler and E. M. Haacke, 2007: Global white matter analysis of diffusion tensor images is predictive of injury severity in traumatic brain injury. *Journal of neurotrauma,* **24,** 446-459.

Berridge, M. J., 1998: Neuronal calcium signaling. *Neuron,* **21,** 13-26.

Blennow, K., J. Hardy and H. Zetterberg, 2012: The neuropathology and neurobiology of traumatic brain injury. *Neuron,* **76,** 886-899.

Bonislawski, D. P., E. P. Schwarzbach and A. S. Cohen, 2007: Brain injury impairs dentate gyrus inhibitory efficacy. *Neurobiology of disease,* **25,** 163-169.

Bootman, M. D. and M. J. Berridge, 1995: The elemental principles of calcium signaling. *Cell,* **83,** 675-678.

Brahmachari, S., Y. K. Fung and K. Pahan, 2006: Induction of glial fibrillary acidic protein expression in astrocytes by nitric oxide. *The Journal of neuroscience : the official journal of the Society for Neuroscience,* **26,** 4930-4939.

Bryant, R., 2011: Post-traumatic stress disorder vs traumatic brain injury. *Dialogues in clinical neuroscience,* **13,** 251-262.

Buck, P. W., 2011: Mild traumatic brain injury: a silent epidemic in our practices. *Health & social work,* **36,** 299-302.

Burgess, P., E. S. E, M. S. S, M. W. M, E. Ossmann and V. Kapil, 2010: Managing traumatic brain injury secondary to explosions. *Journal of emergencies, trauma, and shock,* **3,** 164-172.

Buritica, E., L. Villamil, F. Guzman, M. I. Escobar, N. Garcia-Cairasco and H. J. Pimienta, 2009: Changes in calcium-binding protein expression in human cortical contusion tissue. *Journal of neurotrauma,* **26,** 2145-2155.

Camp, A. J. and R. Wijesinghe, 2009: Calretinin: modulator of neuronal excitability. *The international journal of biochemistry & cell biology,* **41,** 2118-2121.

Carbonell, W. S. and M. S. Grady, 1999: Regional and temporal characterization of neuronal, glial, and axonal response after traumatic brain injury in the mouse. *Acta neuropathologica,* **98,** 396-406.

Carey, M. E., G. S. Sarna, J. B. Farrell and L. T. Happel, 1989: Experimental missile wound to the brain. *Journal of neurosurgery,* **71,** 754-764.

Cernak, I., 2005: Animal models of head trauma. *NeuroRx : the journal of the American Society for Experimental NeuroTherapeutics,* **2,** 410-422.

Cernak, I. and L. J. Noble-Haeusslein, 2010: Traumatic brain injury: an overview of pathobiology with emphasis on military populations. *Journal of cerebral blood flow and metabolism : official journal of the International Society of Cerebral Blood Flow and Metabolism,* **30,** 255-266.

Cernak, I., J. Savic, D. Ignjatovic and M. Jevtic, 1999: Blast injury from explosive munitions. *The Journal of trauma,* **47,** 96-103; discussion 103-104.

Cheng, C. L. and J. T. Povlishock, 1988: The effect of traumatic brain injury on the visual system: a morphologic characterization of reactive axonal change. *Journal of neurotrauma,* **5,** 47-60.

Clemedson, C. J., 1956: Blast injury. *Physiological reviews,* **36,** 336-354.

Cockerham, G. C., G. L. Goodrich, E. D. Weichel, J. C. Orcutt, J. F. Rizzo, K. S. Bower and R. A. Schuchard, 2009: Eye and visual function in traumatic brain injury. *Journal of rehabilitation research and development,* **46,** 811-818.

Curtis, M. A., E. B. Penney, A. G. Pearson, W. M. van Roon-Mom, N. J. Butterworth, M. Dragunow, B. Connor and R. L. Faull, 2003: Increased cell proliferation and neurogenesis in the adult human Huntington's disease brain. *Proceedings of the National Academy of Sciences of the United States of America,* **100,** 9023-9027.

D'Orlando, C., M. R. Celio and B. Schwaller, 2002: Calretinin and calbindin D-28k, but not parvalbumin protect against glutamate-induced delayed excitotoxicity in transfected N18-RE 105 neuroblastoma-retina hybrid cells. *Brain research,* **945,** 181-190.

Dash, P. K., S. A. Mach and A. N. Moore, 2001: Enhanced neurogenesis in the rodent hippocampus following traumatic brain injury. *Journal of neuroscience research,* **63,** 313-319.

Denny-Brown, D., 1945: Cerebral concussion. *Physiological reviews,* **25**.

DePalma, R. G., D. G. Burris, H. R. Champion and M. J. Hodgson, 2005: Blast injuries. *The New England journal of medicine,* **352,** 1335-1342.

Deshpande, L. S., D. A. Sun, S. Sombati, A. Baranova, M. S. Wilson, E. Attkisson, R. J. Hamm and R. J. DeLorenzo, 2008: Alterations in neuronal calcium levels are associated with cognitive deficits after traumatic brain injury. *Neuroscience letters,* **441,** 115-119.

Dickson, D., 1943: Blast in 1812. *Lancet,* **1,** 1.

Dixon, C. E., B. G. Lyeth, J. T. Povlishock, R. L. Findling, R. J. Hamm, A. Marmarou, H. F. Young and R. L. Hayes, 1987: A fluid percussion model of experimental brain injury in the rat. *Journal of neurosurgery,* **67,** 110-119.

Feeney, D. M., M. G. Boyeson, R. T. Linn, H. M. Murray and W. G. Dail, 1981: Responses to cortical injury: I. Methodology and local effects of contusions in the rat. *Brain research,* **211,** 67-77.

Foda, M. A. and A. Marmarou, 1994: A new model of diffuse brain injury in rats. Part II: Morphological characterization. *Journal of neurosurgery,* **80,** 301-313.

Franklin, B. J. and G. Paxinos, 2008: *The Mouse Brain in Stereotaxic Coordinates*. Academic Press.

Freund, T. F., G. Buzsaki, A. Leon, K. G. Baimbridge and P. Somogyi, 1990: Relationship of neuronal vulnerability and calcium binding protein immunoreactivity in ischemia. *Experimental brain research. Experimentelle Hirnforschung. Experimentation cerebrale,* **83,** 55-66.

Fulton, J., 1942: Blast and concussion in the present war. *The New England journal of medicine,* **226,** 8.

Gao, X., Y. Deng-Bryant, W. Cho, K. M. Carrico, E. D. Hall and J. Chen, 2008: Selective death of newborn neurons in hippocampal dentate gyrus following moderate experimental traumatic brain injury. *Journal of neuroscience research,* **86,** 2258-2270.

Geddes, D. M., M. C. LaPlaca and R. S. Cargill, 2nd, 2003: Susceptibility of hippocampal neurons to mechanically induced injury. *Experimental neurology,* **184,** 420-427.

Glaesser, J., F. Neuner, R. Lutgehetmann, R. Schmidt and T. Elbert, 2004: Posttraumatic Stress Disorder in patients with traumatic brain injury. *BMC psychiatry,* **4,** 5.

Goodrich, G. L., G. L. Martinsen, H. M. Flyg, J. Kirby, S. M. Asch, K. D. Brahm, J. M. Brand, D. Cajamarca, J. L. Cantrell, T. Chong, J. A. Dziadul, B. J. Hetrick, M. A. Huang, C. Ihrig, S. P. Ingalla, B. R. Meltzer, C. M. Rakoczy, A. Rone, E. Schwartz and J. E. Shea, 2013: Development of a mild traumatic brain injury-specific vision screening protocol: a Delphi study. *Journal of rehabilitation research and development,* **50,** 757-768.

Greve, M. W. and B. J. Zink, 2009: Pathophysiology of traumatic brain injury. *The Mount Sinai journal of medicine, New York,* **76,** 97-104.

Grote, S., W. Bocker, W. Mutschler, B. Bouillon and R. Lefering, 2011: Diagnostic value of the Glasgow Coma Scale for traumatic brain injury in 18,002 patients with severe multiple injuries. *Journal of neurotrauma,* **28,** 527-534.

Isaacs, K. R., M. E. Wolpoe and D. M. Jacobowitz, 2000: Vulnerability to calcium-induced neurotoxicity in cultured neurons expressing calretinin. *Experimental neurology,* **163,** 311-323.

Jars, M., 1768: Observations sur la circulation de la'air dans les mines: Moyens qu'il faut employer pour l'y maintenir. Second mémoire. . *Hist. de l'Acad. Roy. Sci. Mem. de Math. et Phys.*

Jin, K., V. Galvan, L. Xie, X. O. Mao, O. F. Gorostiza, D. E. Bredesen and D. A. Greenberg, 2004: Enhanced neurogenesis in Alzheimer's disease transgenic (PDGF-APPSw,Ind) mice. *Proceedings of the National Academy of Sciences of the United States of America,* **101,** 13363-13367.

Jin, K., X. Wang, L. Xie, X. O. Mao, W. Zhu, Y. Wang, J. Shen, Y. Mao, S. Banwait and D. A. Greenberg, 2006: Evidence for stroke-induced neurogenesis in the human brain. *Proceedings of the National Academy of Sciences of the United States of America,* **103,** 13198-13202.

Jones, E., 2006: Historical approaches to post-combat disorders. *Philosophical transactions of the Royal Society of London. Series B, Biological sciences,* **361,** 533-542.

Jones, E., N. T. Fear and S. Wessely, 2007: Shell shock and mild traumatic brain injury: a historical review. *The American journal of psychiatry,* **164,** 1641-1645.

Kamnaksh, A., E. Kovesdi, S. K. Kwon, D. Wingo, F. Ahmed, N. E. Grunberg, J. Long and D. V. Agoston, 2011: Factors affecting blast traumatic brain injury. *Journal of neurotrauma,* **28,** 2145-2153.

Kan, E. M., E. A. Ling and J. Lu, 2012: Microenvironment changes in mild traumatic brain injury. *Brain research bulletin,* **87,** 359-372.

Kapoor, N. and K. J. Ciuffreda, 2002: Vision Disturbances Following Traumatic Brain Injury. *Current treatment options in neurology,* **4,** 271-280.

Kempermann, G. and F. H. Gage, 2000: Neurogenesis in the adult hippocampus. *Novartis Foundation symposium,* **231,** 220-235; discussion 235-241, 302-226.

Kernie, S. G. and J. M. Parent, 2010: Forebrain neurogenesis after focal Ischemic and traumatic brain injury. *Neurobiology of disease,* **37,** 267-274.

Kim, J. J. and A. D. Gean, 2011: Imaging for the diagnosis and management of traumatic brain injury. *Neurotherapeutics : the journal of the American Society for Experimental NeuroTherapeutics,* **8,** 39-53.

Kuehn, R., P. F. Simard, I. Driscoll, K. Keledjian, S. Ivanova, C. Tosun, A. Williams, G. Bochicchio, V. Gerzanich and J. M. Simard, 2011: Rodent model of direct cranial blast injury. *Journal of neurotrauma,* **28,** 2155-2169.

Lighthall, J. W., H. G. Goshgarian and C. R. Pinderski, 1990: Characterization of axonal injury produced by controlled cortical impact. *Journal of neurotrauma,* **7,** 65-76.

Liu, D., C. L. Smith, F. C. Barone, J. A. Ellison, P. G. Lysko, K. Li and I. A. Simpson, 1999: Astrocytic demise precedes delayed neuronal death in focal ischemic rat brain. *Brain research. Molecular brain research,* **68,** 29-41.

Longhi, L., K. E. Saatman, R. Raghupathi, H. L. Laurer, P. M. Lenzlinger, P. Riess, E. Neugebauer, J. Q. Trojanowski, V. M. Lee, M. S. Grady, D. I. Graham and T. K. McIntosh, 2001: A review and rationale for the use of genetically engineered animals in the study of traumatic brain injury. *Journal of cerebral blood flow and metabolism : official journal of the International Society of Cerebral Blood Flow and Metabolism,* **21,** 1241-1258.

Lowenstein, D. H., M. J. Thomas, D. H. Smith and T. K. McIntosh, 1992: Selective vulnerability of dentate hilar neurons following traumatic brain injury: a potential mechanistic link between head trauma and disorders of the hippocampus. *The Journal of neuroscience : the official journal of the Society for Neuroscience,* **12,** 4846-4853.

Markgraf, C. G., G. L. Clifton, M. Aguirre, S. F. Chaney, C. Knox-Du Bois, K. Kennon and N. Verma, 2001: Injury severity and sensitivity to treatment after controlled cortical impact in rats. *Journal of neurotrauma,* **18,** 175-186.

Marmarou, A., M. A. Foda, W. van den Brink, J. Campbell, H. Kita and K. Demetriadou, 1994: A new model of diffuse brain injury in rats. Part I: Pathophysiology and biomechanics. *Journal of neurosurgery,* **80,** 291-300.

Matthews, M. A., M. E. Carey, J. S. Soblosky, J. F. Davidson and S. L. Tabor, 1998: Focal brain injury and its effects on cerebral mantle, neurons, and fiber tracks. *Brain research,* **794,** 1-18.

Mattson, M. P., 2008: Glutamate and neurotrophic factors in neuronal plasticity and disease. *Annals of the New York Academy of Sciences,* **1144,** 97-112.

Mayorga, M. A., 1997: The pathology of primary blast overpressure injury. *Toxicology,* **121,** 17-28.

McCarthy, M. M., 2003: Stretching the truth. Why hippocampal neurons are so vulnerable following traumatic brain injury. *Experimental neurology,* **184,** 40-43.

Middeldorp, J. and E. M. Hol, 2011: GFAP in health and disease. *Progress in neurobiology,* **93,** 421-443.

Miller, R. J., 1991: The control of neuronal Ca2+ homeostasis. *Progress in neurobiology,* **37,** 255-285.

Moore, D. F., Radovitzy, R.A., Shupenko L., Klinoff A., Jaffee M.S., Rosen J.M., 2008: Blast physics and central nervous system injury. *Future Neurology,* **3,** 243-250.

Morales, D. M., N. Marklund, D. Lebold, H. J. Thompson, A. Pitkanen, W. L. Maxwell, L. Longhi, H. Laurer, M. Maegele, E. Neugebauer, D. I. Graham, N. Stocchetti and T. K. McIntosh, 2005: Experimental models of traumatic brain injury: do we really need to build a better mousetrap? *Neuroscience,* **136,** 971-989.

Morganti-Kossmann, M. C., E. Yan and N. Bye, 2010: Animal models of traumatic brain injury: is there an optimal model to reproduce human brain injury in the laboratory? *Injury,* **41 Suppl 1,** S10-13.

Mott, F., 1916: The effects of high explosives on the central nervous system. . *Lancet,* **1**.

Myer, D. J., G. G. Gurkoff, S. M. Lee, D. A. Hovda and M. V. Sofroniew, 2006: Essential protective roles of reactive astrocytes in traumatic brain injury. *Brain : a journal of neurology,* **129,** 2761-2772.

NIH-NINDS, 2013: Traumatic Brain Injury: Hope Through Research.

O'Connor, W. T., A. Smyth and M. D. Gilchrist, 2011: Animal models of traumatic brain injury: a critical evaluation. *Pharmacology & therapeutics,* **130,** 106-113.

Pandit, A. S., P. Expert, R. Lambiotte, V. Bonnelle, R. Leech, F. E. Turkheimer and D. J. Sharp, 2013: Traumatic brain injury impairs small-world topology. *Neurology,* **80,** 1826-1833.

Parron, C. and E. Save, 2004: Comparison of the effects of entorhinal and retrosplenial cortical lesions on habituation, reaction to spatial and non-spatial changes during object exploration in the rat. *Neurobiology of learning and memory,* **82,** 1-11.

Pierce, J. E., D. H. Smith, J. Q. Trojanowski and T. K. McIntosh, 1998: Enduring cognitive, neurobehavioral and histopathological changes persist for up to one year following severe experimental brain injury in rats. *Neuroscience,* **87,** 359-369.

Pong, W. W., R. Stouracova, N. Frank, J. P. Kraus and W. D. Eldred, 2007: Comparative localization of cystathionine beta-synthase and cystathionine gamma-lyase in retina: differences between amphibians and mammals. *The Journal of comparative neurology,* **505,** 158-165.

Ritenour, A. E. and T. W. Baskin, 2008: Primary blast injury: update on diagnosis and treatment. *Critical care medicine,* **36,** S311-317.

Ropper, A., 2011: Brain injuries from blasts. *The New England journal of medicine,* **364,** 2156-2157.

Rosenfeld, J. V., A. C. McFarlane, P. Bragge, R. A. Armonda, J. B. Grimes and G. S. Ling, 2013: Blast-related traumatic brain injury. *Lancet neurology,* **12,** 882-893.

Rowe, R. K., J. L. Harrison, T. C. Thomas, J. R. Pauly, P. D. Adelson and J. Lifshitz, 2013: Using anesthetics and analgesics in experimental traumatic brain injury. *Lab animal,* **42,** 286-291.

Ruff, R. M., G. L. Iverson, J. T. Barth, S. S. Bush, D. K. Broshek, N. A. N. Policy and C. Planning, 2009: Recommendations for diagnosing a mild traumatic brain injury: a National Academy of Neuropsychology education paper. *Archives of clinical neuropsychology : the official journal of the National Academy of Neuropsychologists,* **24,** 3-10.

Scharfman, H. E. and C. E. Myers, 2012: Hilar mossy cells of the dentate gyrus: a historical perspective. *Frontiers in neural circuits,* **6,** 106.

Schifilliti, D., G. Grasso, A. Conti and V. Fodale, 2010: Anaesthetic-related neuroprotection: intravenous or inhalational agents? *CNS drugs,* **24,** 893-907.

Schwaller, B., 2009: The continuing disappearance of "pure" Ca2+ buffers. *Cellular and molecular life sciences : CMLS,* **66,** 275-300.

Schwaller, B., 2010: Cytosolic Ca2+ buffers. *Cold Spring Harbor perspectives in biology,* **2,** a004051.

Sgubin, D., E. Aztiria, A. Perin, P. Longatti and G. Leanza, 2007: Activation of endogenous neural stem cells in the adult human brain following subarachnoid hemorrhage. *Journal of neuroscience research,* **85,** 1647-1655.

Shi, J., D. K. Miles, B. A. Orr, S. M. Massa and S. G. Kernie, 2007: Injury-induced neurogenesis in Bax-deficient mice: evidence for regulation by voltage-gated potassium channels. *The European journal of neuroscience,* **25,** 3499-3512.

Shohami, E., Y. Shapira and S. Cotev, 1988: Experimental closed head injury in rats: prostaglandin production in a noninjured zone. *Neurosurgery,* **22,** 859-863.

Smith, D. H., R. Hicks and J. T. Povlishock, 2013: Therapy development for diffuse axonal injury. *Journal of neurotrauma,* **30,** 307-323.

Smith, D. H., Meaney, D.F., 2000: Axonal Damage in Traumatic Brain Injury. *Progress in Clinical Neuroscience,* **6,** 483-495.

Sofroniew, M. V., 2009: Molecular dissection of reactive astrogliosis and glial scar formation. *Trends in neurosciences,* **32,** 638-647.

Sosa, M. A., R. De Gasperi, A. J. Paulino, P. E. Pricop, M. C. Shaughness, E. Maudlin-Jeronimo, A. A. Hall, W. G. Janssen, F. J. Yuk, N. P. Dorr, D. L. Dickstein, R. M. McCarron, M. Chavko, P. R. Hof, S. T. Ahlers and G. A. Elder, 2013: Blast overpressure induces shear-related injuries in the brain of rats exposed to a mild traumatic brain injury. *Acta neuropathologica communications,* **1,** 51.

Statler, K. D., H. Alexander, V. Vagni, C. E. Dixon, R. S. Clark, L. Jenkins and P. M. Kochanek, 2006: Comparison of seven anesthetic agents on outcome after experimental traumatic brain injury in adult, male rats. *Journal of neurotrauma,* **23,** 97-108.

Stringer, J. L., 1996: Repeated seizures increase GFAP and vimentin in the hippocampus. *Brain research,* **717,** 147-153.

Stuhmiller, J. H., 1997: Biological response to blast overpressure: a summary of modeling. *Toxicology,* **121,** 91-103.

Sun, D., M. J. McGinn, Z. Zhou, H. B. Harvey, M. R. Bullock and R. J. Colello, 2007: Anatomical integration of newly generated dentate granule neurons following traumatic brain injury in adult rats and its association to cognitive recovery. *Experimental neurology,* **204,** 264-272.

Svetlov, S. I., S. F. Larner, D. R. Kirk, J. Atkinson, R. L. Hayes and K. K. Wang, 2009: Biomarkers of blast-induced neurotrauma: profiling molecular and cellular mechanisms of blast brain injury. *Journal of neurotrauma,* **26,** 913-921.

Sword, J., T. Masuda, D. Croom and S. A. Kirov, 2013: Evolution of neuronal and astroglial disruption in the peri-contusional cortex of mice revealed by in vivo two-photon imaging. *Brain : a journal of neurology,* **136,** 1446-1461.

Toader, O., N. Forte, M. Orlando, E. Ferrea, A. Raimondi, P. Baldelli, F. Benfenati and L. Medrihan, 2013: Dentate gyrus network dysfunctions precede the symptomatic phase in a genetic mouse model of seizures. *Frontiers in cellular neuroscience,* **7,** 138.

Torre, E. R., E. Lothman and O. Steward, 1993: Glial response to neuronal activity: GFAP-mRNA and protein levels are transiently increased in the hippocampus after seizures. *Brain research,* **631,** 256-264.

Urrea, C., D. A. Castellanos, J. Sagen, P. Tsoulfas, H. M. Bramlett and W. D. Dietrich, 2007: Widespread cellular proliferation and focal neurogenesis after traumatic brain injury in the rat. *Restorative neurology and neuroscience,* **25,** 65-76.

Vakil, E., 2005: The effect of moderate to severe traumatic brain injury (TBI) on different aspects of memory: a selective review. *Journal of clinical and experimental neuropsychology,* **27,** 977-1021.

Vann, S. D., J. P. Aggleton and E. A. Maguire, 2009: What does the retrosplenial cortex do? *Nature reviews. Neuroscience,* **10,** 792-802.

Weber, J. T., 2012: Altered calcium signaling following traumatic brain injury. *Frontiers in pharmacology,* **3,** 60.

Weber, J. T., B. A. Rzigalinski and E. F. Ellis, 2001: Traumatic injury of cortical neurons causes changes in intracellular calcium stores and capacitative calcium influx. *The Journal of biological chemistry,* **276,** 1800-1807.

Wintermark, M., G. van Melle, P. Schnyder, J. P. Revelly, F. Porchet, L. Regli, R. Meuli, P. Maeder and R. Chiolero, 2004: Admission perfusion CT: prognostic value in patients with severe head trauma. *Radiology,* **232,** 211-220.

Wolf, S. J., V. S. Bebarta, C. J. Bonnett, P. T. Pons and S. V. Cantrill, 2009: Blast injuries. *Lancet,* **374,** 405-415.

Wyss, J. M. and T. Van Groen, 1992: Connections between the retrosplenial cortex and the hippocampal formation in the rat: a review. *Hippocampus,* **2,** 1-11.

Xiong, Y., A. Mahmood and M. Chopp, 2013: Animal models of traumatic brain injury. *Nature reviews. Neuroscience,* **14,** 128-142.

Yount, R., K. A. Raschke, M. Biru, D. F. Tate, M. J. Miller, T. Abildskov, P. Gandhi, D. Ryser, R. O. Hopkins and E. D. Bigler, 2002: Traumatic brain injury and atrophy of the cingulate gyrus. *The Journal of neuropsychiatry and clinical neurosciences,* **14,** 416-423.

Yu, T. S., G. Zhang, D. J. Liebl and S. G. Kernie, 2008: Traumatic brain injury-induced hippocampal neurogenesis requires activation of early nestin-expressing progenitors. *The Journal of neuroscience : the official journal of the Society for Neuroscience,* **28,** 12901-12912.

Zhao, X., A. Ahram, R. F. Berman, J. P. Muizelaar and B. G. Lyeth, 2003: Early loss of astrocytes after experimental traumatic brain injury. *Glia,* **44,** 140-152.

Zheng, W., Q. Zhuge, M. Zhong, G. Chen, B. Shao, H. Wang, X. Mao, L. Xie and K. Jin, 2013: Neurogenesis in adult human brain after traumatic brain injury. *Journal of neurotrauma,* **30,** 1872-1880.